UNIVERSITAT POLITÈCNICA DE VALÈNCIA

ULB BRUFACE BRUSSELS FACULTY OF ENGINEERING VUB

Master's Thesis

Conceptual design of a Boeing ScanEagle drone using H2 propulsion

Author:

Elfidio Ángel Alonso Artal

Thesis supervisors:

Prof. Dr. Ir. Patrick Hendrick

Dr. Ir. Marcos López Juárez

Master's Degree in Aeronautical Engineering

Academic year 2022-2023

ULB UNIVERSITÉ LIBRE DE BRUXELLES

ULB UNIVERSITÉ LIBRE DE BRUXELLES

Exemplaire à apposer sur le mémoire ou travail de fin d'études,
au verso de la première page de couverture.

Réservé au secrétariat :	**Mémoire réussi***	**OUI**
		NON

CONSULTATION DU MEMOIRE/TRAVAIL DE FIN D'ETUDES

Je soussigné

NOM :
Alonso Artal
……

PRENOM :
Elfidio Ángel
……..

TITRE du travail : Conceptual design of a Boeing ScanEagle drone using H2 propulsion
……

……
……

AUTORISE*

REFUSE*

la consultation du présent mémoire/travail de fin d'études par les utilisateurs des bibliothèques de l'Université libre de Bruxelles.

Si la consultation est autorisée, le soussigné concède par la présente à l'Université libre de Bruxelles, pour toute la durée légale de protection de l'œuvre, une licence gratuite et non exclusive de reproduction et de communication au public de son œuvre précisée ci-dessus, sur supports graphiques ou électroniques, afin d'en permettre la consultation par les utilisateurs des bibliothèques de l'ULB et d'autres institutions dans les limites du prêt inter-bibliothèques.

Fait en deux exemplaires, **Bruxelles, le** 07/08/2023

Signature

Formulaire version 04/2015

** Biffer la mention inutile*

** Biffer la mention inutile*

Acknowledgements

I would like to express my deepest gratitude to all the individuals who have supported and motivated me during these years of my academic journey, pushing me to keep working and to evolve both academically and personally.

I want to thank my family for their unconditional support during these past years, and especially my mother, who has educated me and paved the way for me to become the person I am today.

To Lau, for being by my side during the toughest moments and sharing with me the best days of these past years.

To Patrick Hendrick and Marcos López, for their patience, professionalism, and immense dedication; to P. Hendrick not only as the project advisor but also as a professor. It has been a pleasure.

And, in general, to all the people I have interacted with during this period; whether inside or outside the university, in both Valencia and Brussels, who have turned these last years into an unforgettable experience.

Abstract

Master's Thesis: Conceptual design of a *Boeing ScanEagle* drone using H_2 propulsion
Author: Elfidio Ángel Alonso Artal
In order to be awarded the Master's Degree in Electromechanical Engineering (Aeronautics)
Academic year 2022-2023

This study has as its main objective the analysis of the application of a hydrogen fuel cell as the main propulsion system for an unmanned aerial vehicle, specifically the *ScanEagle*. The aim is to meet the essential goals of a typical reconnaissance mission. The study begins by reverse engineering the original vehicle to gather information regarding its geometry, weight, propulsion and aerodynamics, followed by programming a simulation of the cruise flight to assess its performance. Once this is accomplished, the new propulsion system is implemented. It is sized during the ascent and cruise phases through an iterative process. The study concludes with a comparison of five different models with varying performance, weights and geometries.

The results demonstrate that none of the designed models can simultaneously fulfill all the objectives of the original mission because of an increase in takeoff weight and size. However, each of them could be used for a modified and specific mission that meet some of these requirements, establishing this new carbon-free technology as a potential replacement for internal combustion engines in UAV applications.

Key words: UAV, drone, PEMFC, hydrogen, ScanEagle, zero emissions.

Contents

Nomenclature

Acronyms

$UAV(s)$ Unmanned Aerial Vehicle(s)

$SAF(s)$ Sustainable Aviation Fuel(s)

$VTOL$ Vertical TakeOff and Landing

$PEMFC$ Proton Exchange Membrane Fuel Cell

IC Internal Combustion

FC Fuel Cell

LHV Lower Heating Value

AoA Angle of Attack

ADS Aircraft Design Software (by OAD)

CAD Computer Aided Design

MAC Mean Aerodynamic Chord

AC Aerodynamic Center

PL Payload

TAS True Air Speed

SL Sea Level

AE Aerodynamic Efficiency

$PEMFC$ Proton Exchange Membrane Fuel Cell

Latin symbols

S	Surface	m^2
b	Wing span	m

AR	Aspect ratio	
c	Chord	m
l	Length	m
d	Diameter (maximum)	m
AC	Aerodynamic Center	m
t	Airfoil thickness w.r.t the chord	m
x	Airfoil longitudinal coordinate w.r.t the chord	m
C_l	Airfoil 2D lift coefficient	
C_d	Airfoil 2D drag coefficient	
C_{l_α}	Airfoil 2D lift coefficient vs AoA line slope	$1/^\circ$
R_e	Reynolds number	
P	Power	W
SFC	(Power) Specific Fuel Consumption	kg/W/s
$MTOW$	Maximum TakeOff Weight	kg
TOW	TakeOff Weight	kg
OEW	Operational Empty Weight	kg
TEW	Total Empty Weight	kg
W	Aircraft weight (mass units)	kg
g	Acceleration of gravity	m/s^2
pi	Propeller pitch	m
ω	Rotational speed	rad/s
V	Aircraft speed (TAS)	m/s
z	Aircraft altitude	m
a	Speed of sound	m/s
M	Mach number	
C_P	Engine power coefficient	

C_T	Engine thrust coefficient	
J_{prop}	Propeller advance ratio	
C_D	Wing 3D drag coefficient	
C_L	Wing 3D lift coefficient	
C_{L_α}	Wing 3D lift coefficient vs AoA line slope	$1/^\circ$
$C_{L_{\alpha=0}}$	Wing 3D lift coefficient for zero AoA	
C_{D_0}	3D Base (zero-lift) drag coefficient	
C_{D_i}	Wing 3D induced (due to lift) drag coefficient	
k	Constant (see specific subscript)	
C_f	Skin friction coefficient	
F	Form factor	
Q	Interference factor	
e	Oswald's factor	
AE	Aerodynamic efficiency	
R	Aircraft range	km
E	Aircraft endurance	h
WL	Wing loading	N/m^2
C_g	Gravimetric capacity	kWh/kg
C_v	Volumetric capacity	kWh/L
v	Volume	L
$\dot{m}$	Mass flow rate	kg/h
J_{bat}	Energy stored in the battery	kWh
t_{climb}	Time needed for the ascent	min

Greek Symbols

λ	Taper ratio	
Λ	Sweep angle	$^\circ$

Γ	Dihedral angle	$^\circ$
α	Angle of attack	$^\circ$
η	Efficiency	
ρ	Air density	kg/m^3
ν	Air kinematic viscosity	m^2/s
μ	Air dynamic viscosity	$kg/m/s$
β	Effective Mach parameter	

Subscripts

w	Wing-related
wet	Wetted
rt	At the root
tip	At the tip
mac	At the Mean Aerodynamic Chord
f	Fuselage-related
t	Tail-related (V-tail)
$winglet$	Winglet-related (projection over the wingspan)
max	At maximum
$minD$	For minimum drag
$minP$	For minimum power
$maxR$	For maximum range
$maxE$	For maximum endurance
cr	At cruise
sh	Shaft-related
PL	Payload-related
acc	Accessories-related
to	At takeoff

LE	At the leading edge
$c/2$	At the half chord
$c/4$	At the quarter chord
$stall$	At stall
$,2D$	Airfoil or 2D-related
$prop$	Propeller-related
$0L$	For zero-lift
1	Takeoff-related
2	Climb-related
3	Cruise-related
4	Landing-related
$,fuel$	Fuel-related
tot	Total
use	Usable
$,in$	Initial
$,fi$	Final
$visc$	Due to viscous losses
ind	Induced-drag-related
sl	At sea level
eff	Effective
suc	Related to leading edge suction parameter
$tank$	Related to the fuel tank
$elec$	Related to the electric power
fc	Related to the fuel cell
$DCDC$	Related to the DC/DC inverter
bat	Related to the battery

mot Related to the electric motor

H_2 Related to hydrogen fuel

climb Related to the climb phase

req Related to the power required for the ascent

av Related to the available power for the ascent

struc Related to the aircraft's structure

extra Related to the aircraft's extra/auxiliary components

rated Related to the rated power for a certain component

propul Related to the propulsion system

List of Figures

List of Tables

Chapter 1

Thesis approach

1 Introduction

Unmanned Aerial Vehicles (UAVs), sometimes known as drones, have risen in popularity across a wide range of industries due to their agility and ability to do tasks that would be difficult or dangerous for human pilots. The *ScanEagle* drone, in particular, has been frequently used for intelligence, surveillance, and reconnaissance activities in both military and civilian environments. However, like many UAVs, its reliance on traditional fossil fuels has raised concerns about its environmental impact and sustainability.

To address these challenges, this thesis investigates the conceptual design of a *ScanEagle* drone with a hydrogen-powered propulsion system. Because of its high energy content and potential for zero-emission operations, hydrogen has been recognized as a prospective replacement to fossil fuels. The use of H_2 as a fuel source can drastically lower the carbon footprint of UAVs while also increasing their overall efficiency.

The purpose of this thesis is to evaluate the technical feasibility and performance of the proposed design, as well as the impact of the hydrogen propulsion system on the drone's weight, endurance, and geometrical characteristics. The research will also look at the benefits and drawbacks of utilizing hydrogen as a fuel source for UAVs in general.

Overall, the goal of this report is to contribute to research on this topic and establish whether this sort of propulsion has the potential to revolutionize the UAV industry by providing a more sustainable and environmentally friendly option for aerial operations. This approach also generates fewer thermal and acoustic emissions, which is useful for military applications [31].

2 Justification and state of the art

For a variety of reasons, sustainable fuels such as hydrogen will become increasingly significant over the next decade. As a result of population growth and industrial expansion, global energy consumption is expected to skyrocket in the next years. As a result, there will be a larger need to develop alternative and sustainable energy sources capable of satisfying this growing demand without negatively impacting the environment.

Secondly, the negative environmental impact of traditional fossil fuels is becoming increasingly apparent. The use of fossil fuels has been linked to climate change, air pollution, and other environmental issues, which can have serious consequences for human health and well-being. A move to more sustainable energy sources is thus crucial for mitigating these negative impacts and ensuring a more environmentally friendly future.

Thirdly, as a result of technology advances and increased demand for renewable energy sources, the energy industry is undergoing significant shifts. Sustainable fuels are a feasible alternative to traditional fossil fuels since they have a lower carbon impact and may be produced from renewable sources such as wind, solar, or hydroelectric power. This allows for a more diversified and sustainable energy mix, which improves energy security and resilience.

This is why, in the next decades, the use of sustainable aviation fuels (SAFs) will be crucial, as it will help address the issues of meeting expanding energy demand while reducing the negative environmental impact of existing fossil fuels. By investing in sustainable fuels and technologies, we can ensure a more sustainable and resilient energy future for generations to come [8].

2.1 Some existing UAVs with H2 fuel cells

There have been several attempts to hydrogen-powered drones since the last decade. Some of them will be named in order to qualitatively compare them to the *ScanEagle* design (which will be subsequently described) and provide an overall description of their configurations and use of H_2. Since aircraft conceptual design is based on existing know-how, only UAVs driven electrically by propellers will be selected.

NRL's Ion Tiger

Developed by the *U.S Naval research Laboratory* (NRL) in 2009 with its own fuel cell stack using oxygen from the ambient air and hydrogen, either in liquid or gaseous form depending on the specific version. It was designed for stealthy and long endurance operations, reaching the 23 hour endurance mark. Its fuel cell stack is made from titanium plates with 3D metal printing technology and it is powered by a single PEMFC [32]. In addition, the compressed gaseous hydrogen is contained in a carbon over wrapped aluminum pressure vessel.

Figure 1.1: *Ion Tiger* drone [32].

As it will be seen later, this drone presents a different configuration to the *ScanEagle*'s: a double puller propeller on the nose, no winglets and a conventional configuration for vertical and horizontal stabilizers.

H3 Dynamics Hywings UAV

H3 Dynamics is a Singapore-based corporation that includes HES Energy Systems and HUS Unmanned Systems. Its fixed wing UAV is powered by an electric engine and a hydrogen fuel cell technology developed by HES that is 3 to 5 times lighter than Li-Po batteries.

Hywings is a fixed-wing unmanned aerial vehicle that can take off without the need of a catapult. Depending on the variation. This aircraft is provided with the possibility of quick hydrogen bottle refueling (G-version) or quick exchange of hydrogen chemical cartridge (L-version) depending on a chosen variant.

Figure 1.2: *Hywings* drone [27].

Sparkle Tech Eagle plus VTOL

This drone has a VTOL capability thanks its propeller's configuration. It is powered by a hydrogen fuel cell and a battery (for helping during peak power) and its wingspan and length is very similar to the latest version of the *ScanEagle*. It can transport more payload but the endurance is reduced to 5 hours.

Figure 1.3: *Eagle plus* drone [15].

JOUAV DJ25

With a similar design as the previous UAV, this drone has the same VTOL capability, but it is heavier, it has a larger wingspan and can carry a lower amount of payload. However, its maximum endurance is slightly higher than the *Eagle Plus'*.

Figure 1.4: *DJ25* drone [13].

MMC Griflion M8

This VTOL's design is functionally comparable to the last mentioned aircaft, with a construction based on a combination of fixed wings and multi-copter features that allows it to take off and land in locations without a landing strip. It is lighter and can carry more payload than the *JOUAV DJ25* while keeping the same endurance. Depending on the variant, this UAV is fitted with a Li-Po battery or an H1 hydrogen fuel cell system.

Figure 1.5: *Griflion M8* drone [19].

To summarize, their main characteristics will be shown in Table 1.1, that could be helpful in order to obtain an order of magnitude of their geometry and weights for certain flight conditions and performance.

	Ion Tiger	**Hywings**	**Eagle Plus**	**DJ25**	**Griflion M8**
$b_w\ [m]$	5.18	3.30	3.50	4.40	3.75
$S_w\ [m^2]$	1.58	0.79	0.70	1.23	0.94
AR	17.00	13.78	17.50	15.74	15.00
$l_f\ [m]$	2.40	2.27	2.00	2.10	2.15
$d_f\ (max)\ [m]$	0.40	0.35	0.30	0.40	0.30
$W_{empty}\ [kg]$	13.00	5.00	12.50	25.00	10.00
$MTOW\ [kg]$	16.00	7.00	22.50	31.00	22.00
s	0.81	0.71	0.56	0.81	0.45
$W_{PL}\ [kg]$	2.50	1.00	10.00	4.00	10.00
$W_{fuel}\ [kg]$	0.50	1.00	1.50	2.00	2.00
$V_{max}\ [m/s]$	28	27	31	27	30
$E_{max}\ [h]$	24	10	5	6	6
$z_{max}\ [m]$	1100	–	4000	3500	5000
P_{max}	550 W	200 W	500 W	–	–

Table 1.1: Main characteristics for similar aircraft [30][27][15][13][22].

3 Objectives

The objective of this thesis is to perform a conceptual design of the *Boeing ScanEagle* UAV using an electrical propulsion system formed by a Proton Exchange Membrane Fuel Cell (PEMFC) that drives an electrical motor using gaseous hydrogen. A battery will be used as well for complementary purposes. Hydrogen fuel has a higher Lower Heating Value (LHV) and energy per unit of mass than kerosene (33.33 kWh/kg and 12.14 kWh/kg, respectively [17]), so it is a very interesting fuel to be considered. Plus, no carbon emissions are produced. Although, it presents a great drawback in terms of energy per unit of volume.

By this change in the original propulsion system, some requirements have to be met so the drone is able to keep performing the same mission.

System requirements

- Fuel is switched from kerosene to gaseous hydrogen.
- An electric motor has to drive the propeller.

Performance requirements

- The original endurance must not be noticeably compromised. This is approximately $16 - 20\,h$, depending on the mission.
- The original cruise altitude and speed should be kept. This is approximately $5000m$, although it also depends on the mission.
- The drone must carry the same maximum payload. This is approximately $5\,kg$.

Operational requirements

- Possible geometry and/or weight changes must not imply a significant modification in the UAV's launching or landing procedures.

These are critical for the surveillance missions to which this UAV is assigned. Payload is mainly reserved for a radar, camera, sensors, etc. That provide useful information during the loiter phase in which the drone is airborne for a large amount of hours. In addition, keeping as much similar specifications as possible to the original IC *ScanEagle* would imply (hypothetically) a reduction in manufacturing costs. However, it may not be an easy task considering this type of fuel demands a higher storage volume.

Chapter 2

Theoretical and preliminary research

In this chapter, a detailed description of the *ScanEagle* drone will be performed. Starting by the current versions, which are powered by a piston or internal combustion (IC) engine, to the desired fuel cell (FC) hydrogen powered concept that will be designed. Afterwards, a reverse engineering procedure on the IC design can be performed in order to extract useful information and key parameters that can be modified to obtain a similar performance for the FC concept.

1 The IC ScanEagle

The *Boeing ScanEagle* drone is a small, unmanned aerial vehicle built by *Insitu* that is designed for intelligence, surveillance, and reconnaissance missions at low altitude. It has a distinctive, long, slender fuselage with a wingspan of $3.1\,m$ to $4\,m$ and a length of $1.2\,m$ to $2.5\,m$, depending on the specific version. The drone is powered by a two-stroke, liquid-cooled internal combustion engine, which provides a maximum speed of around $40\,m/s$ and a range of up to $2500\,km$.

One of the key factors that make the *ScanEagle* drone unique is its advanced imaging capabilities. Equipped with a high-resolution camera, the drone can capture clear and detailed images and video footage from altitudes of up to $19,500\,ft$. The drone also features a stabilized gimbal, which allows for smooth and precise movements while capturing footage.

Another important feature of the *ScanEagle* drone is its durability and reliability. The drone is built to withstand harsh environmental conditions and it is equipped with advanced avionics systems, including GPS, automatic takeoff and landing, and a fail-safe

recovery system. It has been widely used in military operations around the world, including in Iraq and Afghanistan. Its small size, stealth capabilities, and advanced imaging capabilities make it ideal for intelligence, surveillance, and reconnaissance missions. In addition, the drone's ability to operate for extended periods of time without the need for refueling or maintenance makes it an efficient and cost-effective option for military operations [21].

1.1 Variants

Since its introduction in 2005, several variants have been developed. Some of the most relevant are:

ScanEagle A15

As cann be seen in Figure 2.1, the *ScanEagle* has a propeller on the aft part of the fuselage, a long wingspan with a relatively high sweep angle, that allows the winglets to perform as V-tails and a camera on the front part. All the payload, avionics and navigation equipment is located inside the fuselage. This variant has an optimal feature of carburetor deicing and ice-phobic wing covering [4].

Figure 2.1: *ScanEagle A15* [5].

ScanEagle 2

This version (see Figure 2.2) is aimed to provide persistent daytime and nighttime intelligence, surveillance and reconnaissance (ISR) in extreme environments. It provides a superior operational capability and reliability, with advanced payload options and a faster payload integration [21]. Its geometry is very similar to the *ScanEagle A15*'s.

Figure 2.2: *ScanEagle 2* [28].

ScanEagle 3

This design (see Figure 2.3) can double the payload capacity of the previous variants without compromising the endurance. it increases the operational flexibility by accommodating several payloads at the same time, allowing to collect and analyze more information in a single flight. This version has a different configuration, since it has a lower sweep angle, no winglets and the control surfaces are located at the rear thanks to a tail boom. A newer stability and navigation systems are embarked [20].

Figure 2.3: *ScanEagle 3* [34].

In Table 2.1, a comparison of the different specifications of the variants mentioned above can be seen [1]:

Feature	*ScanEagle A15*	*ScanEagle 2*	*ScanEagle 3*
Cruise speed	$25 - 30\,m/s$	$25 - 35\,m/s$	$30 - 40\,m/s$
Max. speed	$36\,m/s$	$41\,m/s$	$45\,m/s$
Endurance	$12 - 15\,h$	$16 - 20\,h$	$20 - 25\,h$
Service ceiling	$5000\,m$	$5950\,m$	$6100\,m$
Wing span	$3.1\,m$	$3.1\,m$	$4\,m$
Length	$1.2\,m$	$1.71\,m$	$2.3 - 2.5\,m$
Max. Payload	$0.6\,kg$	$5.0\,kg$	$8.6\,kg$
Max. fuel	$5.4\,kg$	$5.5\,kg$	-
MTOW	$18\,kg$	$26.5\,kg$	$36.3\,kg$
OEW	$12\,kg$	$11\,kg$	-
Payload power	-	$150\,W$	$170\,W$
Fuselage diameter	-	$0.2\,m$	-

Table 2.1: Specifications for the different IC *ScanEagles*.

1.2 Propulsion system

IC engine

The piston engine chosen for all current *ScanEagle* applications is the two-stroke *3W-28i* adjusted for jet fuel. A lightweight $1.50\,kg$ and $1.12\,kW$ of power engine which is adapted for driving the 2-blade propeller. This power has to be also distributed to the payload equipment which is chosen by the customer and the onboard avionics [4].

Figure 2.4: *2-stroke 3W-28i IC engine* [35].

Propeller

The propeller used is the *APC* propeller *model LP16014P* [33]. It is a 2-blade propeller made out of resin and chopped fiberglass. It has a 40.64cm diameter and a 35.6cm pitch[1]. Unless it is specified, this propeller will be kept in the new design.

Figure 2.5: *APC LP16014P* propeller [33].

1.3 Takeoff and landing

This drone is not equipped with a landing gear, thus, it does not need a runway in order to takeoff and land. In fact, it is launched by a catapult system (*SuperWedge*) that can be easily transported in large boats or even set up on the ground. This system sends the drone into the air with the needed AoA at 25 m/s. In order to land, the UAV is captured by a *SkyHook* system equipped with a long elastic cable that hangs from a long pole thanks to hook placed at the winglets.

(a) Catapult launch.

(b) Hook landing.

Figure 2.6: Takeoff and landing procedures [18][24].

[1]Describes how far forward in a specific fluid the propeller can move in a single revolution.

1.4 Mission profile

Before starting with the reverse engineering process, it is important to select a mission profile, based on a real possible real case scenario in which the ScanEagle could perform (Figure 2.7).

Since this UAV is originally built and designed for surveillance and reconnaissance activities, the mission profile is simple but quite long. It consists in:

1. **Takeoff**: *Desert Ridge United State's Air Force Base*, located in the outskirts of the city of Tucson, Arizona at 800 m altitude ASL (hypothesis).

2. **Climb and acceleration**: The engine runs at a certain power for the amount of time needed in order to reach the cruise altitude at the desired cruise speed[2].

3. **First Cruise**: The UAV reaches the desired cruise altitude and flies at the cruise (maximum range) velocity for a horizontal distance of 320 km, entering the border region between Arizona and New Mexico, covering a stretch of rugged desert terrain known as the *Cholla Valley*.

4. **Loiter in mission area**: The surveillance and reconnaissance mission begins over *Rattlesnake Ridge*, a series of elevated plateaus overlooking potential smuggling routes, and the *Coyote Pass*, a known hotspot for illicit border crossings. The UAV will fly at the maximum endurance velocity for the vast majority of the time while airborne.

5. **Second Cruise**: The mission has ended and the UAV will come back to the origin site flying a high percentage of the remaining 320 km distance at the cruise (maximum range) velocity.

6. **Descent/Landing**: The UAV will descend from the cruise altitude thanks to its gliding capabilities. So, a percentage of those 320 km back to the origin site will be done by means of an unpowered flight. A 5% of the total fuel would be saved for an emergency.

[2]This amount of time and power needed is not calculated, but its corresponding consumed fuel weight fraction will be assumed according to the bibliography.

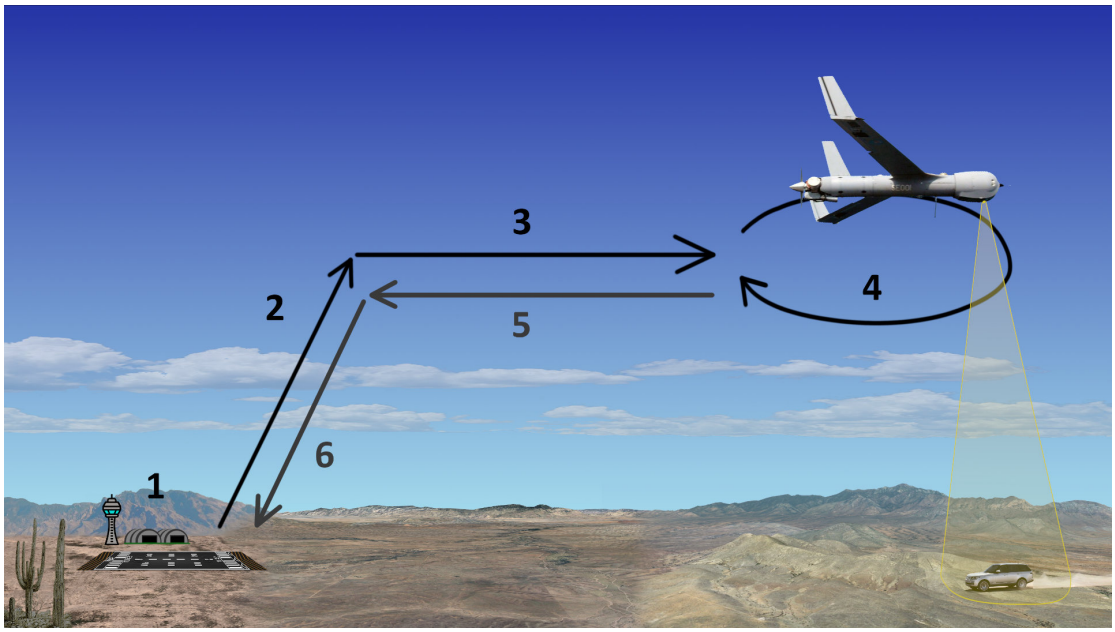

Figure 2.7: Selected mission profile.

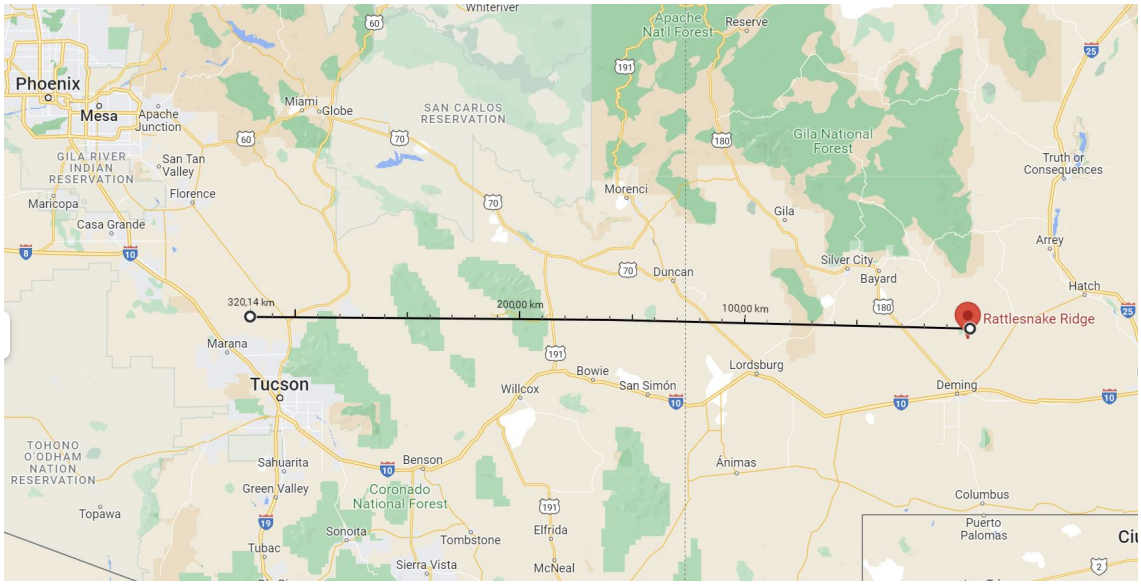

Figure 2.8: Cruise to mission distance (Google Maps).

2 Reverse engineering

In order to obtain as much technical information as possible from the original reciprocating engine (IC) drone, a reverse engineering process is done. This is, gathering and estimating key geometrical and performance parameters that will potentially allow to

design a hydrogen-powered version that meets the requirements stated at chapter 1 - section 3.

The idea is to minimize the number of unknown parameters from the original design, so reasoning and simplifications can be made without compromising the reliability of the calculations. Both Corke's [10] and Raymer's [26] methodologies will be used for this reverse engineering process.

It is important to highlight the fact that the **ScanEagle 2** (Figure 2.2) will be the reference UAV selected, since it is the one from which the largest amount of bibliography has been found. Plus, this version has been widely used and is relatively recent.

2.1 Flight conditions

Because the weight of the aircraft is continually decreasing due to fuel consumption, flight conditions will vary during cruise and loiter. Expendable payload will not be considered.

Velocity, and thus, the Mach number and the dynamic pressure at the cruise altitude will vary. This is because the UAV will fly at the maximum range or maximum endurance speeds only. These two velocities will be obtained by knowing the aircraft weight at every time interval and the corresponding lift coefficient.

The only fixed variable is the cruise altitude, which will be $z = 5000\,m$, knowing that there is a reasonable margin with respect to its flight ceiling. Following the ISA model, the most relevant parameters related to flight conditions are summarized in Table 2.2.

Parameter	**Value**
z_{max}	$5950\,m$
z_{cr}	$5000\,m$
V_{max}	$41\,m/s$
V_{cr}	*variable*
a_{cr}	$320.53\,m/s$
M_{max}	0.13
M_{cr}	*variable*
ρ_{cr}	$0.74\,kg/m^3$
ν_{cr}	$2.21 \cdot 10^{-5}\,m^2/s$
μ_{cr}	$3.00 \cdot 10^{-5}\,kg/(m \cdot s)$
q_{cr}	*variable*

Table 2.2: Cruise flight conditions.

2.2 Estimation of basic geometry

From the information obtained in Table 2.1, and with the help of *OAD'S Aircraft Design Software*[3], it is possible to extract this drone's main dimensions and geometrical parameters.

ADS® is available on the market for aircraft designers, universities, research institutes or even for amateur users. Uploading a scaled 3D view of a specific aircraft, it is possible to create a model using control points and lines in order to simulate a very precise 3D CAD model of the drone. This allows to obtain the remaining unknown values that are required for the reverse engineering, such as the wing surface, aspect ratio, taper ratio, sweep angles, etc.

This software also allows to choose which kind of aircraft is going to be studied (e.g: Unmanned Aerial Vehicle, ultralight and light airplanes, civil transport jet, etc), although it is not prepared for supersonic applications. In addition, the type of propulsion can be selected (e.g: piston engine, turboprop, turbofan, electric.) and also other specific data related to whether the aircraft has landing gear or not, control surfaces, fuel tanks, airfoils, cabin information and many more.

The resulting 3D model can be seen in Figure 2.9:

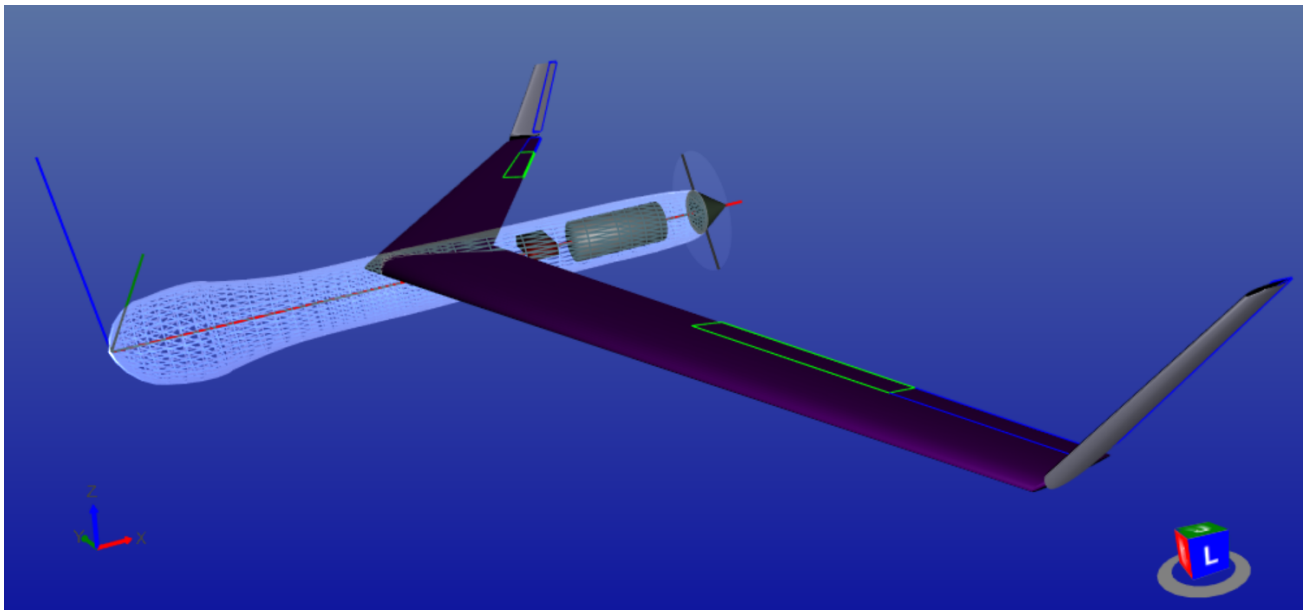

Figure 2.9: IC ScanEagle 2 model in ADS®.

[3]ADS® is a very efficient and useful software aimed for aircraft conceptual and preliminary design.

The values obtained from this model are tabulated in Table 2.3. Since it has been made from scaled images of the original UAV, the resulting geometry can be assumed almost identical to the real aircraft.

Wing	**V-Tail**	**Fuselage**
$S = 0.86\,m^2$	$S = 0.09\,m^2$	$l = 1.71\,m$
$b = 3.11\,m$	$b = 0.63\,m$	$d = 0.20\,m$
$AR = 11.20$	$AR = 4.41$	$S_{wet} = 0.96\,m^2$
$b_{winglet} = 0.39$	$c_{rt} = 0.15\,m$	
$c_{rt} = 0.37\,m$	$c_{tip} = 0.11\,m$	
$c_{tip} = 0.19\,m$	$c_{mac} = 0.13\,m$	
$c_{mac} = 0.29\,m$	$\lambda = 0.71$	
$\lambda = 0.50$	$\Lambda_{LE} = 60.4°$	
$\Lambda_{LE} = 28.4°$	$\Lambda_{c/2} = 57.6°$	
$\Lambda_{c/2} = 25.7°$	$\Lambda_{c/4} = 59.0°$	
$\Lambda_{c/4} = 27.1°$	$\Gamma = 68.2°$	
$\Gamma = -2.4°$		

Table 2.3: IC ScanEagle geometry estimation using ADS®.

As it can be seen in the last figure, this UAV has a V-shaped tail. These control surfaces act as ruddervators[4]. Despite the fact that the ScanEagle is not designed for taking off and landing on a runway, it has flaps. These are part of its control surfaces to adjust its aerodynamic performance during flight. The flaps are located on the trailing edge of the drone's wings and can be extended or retracted to change the lift and drag characteristics of the wings. By adjusting the position of the flaps, the drone can change its speed, altitude, and maneuverability, making it more versatile and adaptable to different mission requirements. Although they are not strictly necessary for increasing lift at low velocities during the landing procedure since the *SkyHook* system absorbs the remaining kinetic of the drone.

2.3 Airfoil selection

Because there is frequently little information available about the airfoil used on an aircraft's main wing and empennage, a decision must be made based on the requirements. As will be shown later in the reverse engineering process, the aircraft's main wing must create enough lift to allow the aircraft to fly at relatively moderate speeds, hence decreasing drag or power when in cruise. Since the associated lift coefficient directly depends on

[4]This type of surfaces provide both pitch and yaw control.

the weight of the aircraft at each time interval, one must take into account that by no means can this lift coefficient be higher than the maximum lift coefficient the 3D wing can provide at that flight condition.

According to this restriction, a 5 digit NACA airfoil has been selected with the following characteristics:

Main wing's airfoil: NACA 44012

This airfoil profile can be seen in Figure 2.10.

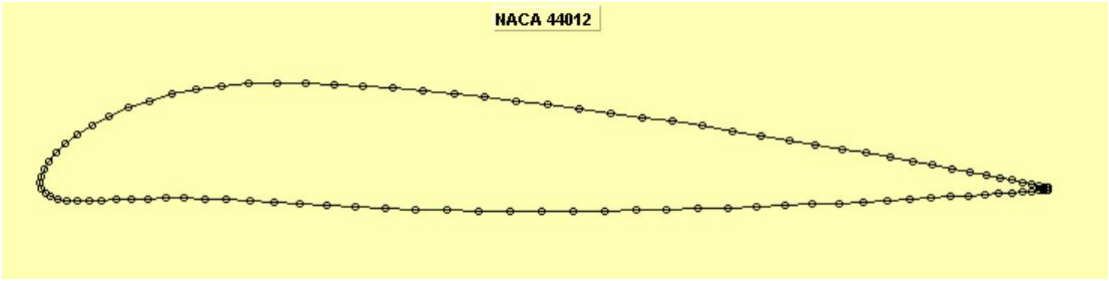

Figure 2.10: NACA 44012 12% airfoil (JavaFoil).

Thanks to *JavaFoil* software, 2D C_l and C_d coefficients at different AoA and Reynolds can be obtained. This allows plotting several curves and calculate the real 3D wing coefficients afterwards.

Some of the relevant curves that can be obtain using the data provided by JavaFoil are the $C_l - \alpha$, $C_d - \alpha$, $C_l - C_d$ and $C_l^{3/2}/C_d - \alpha$ curves, respectively in Figure 2.11 and Figure 2.12.

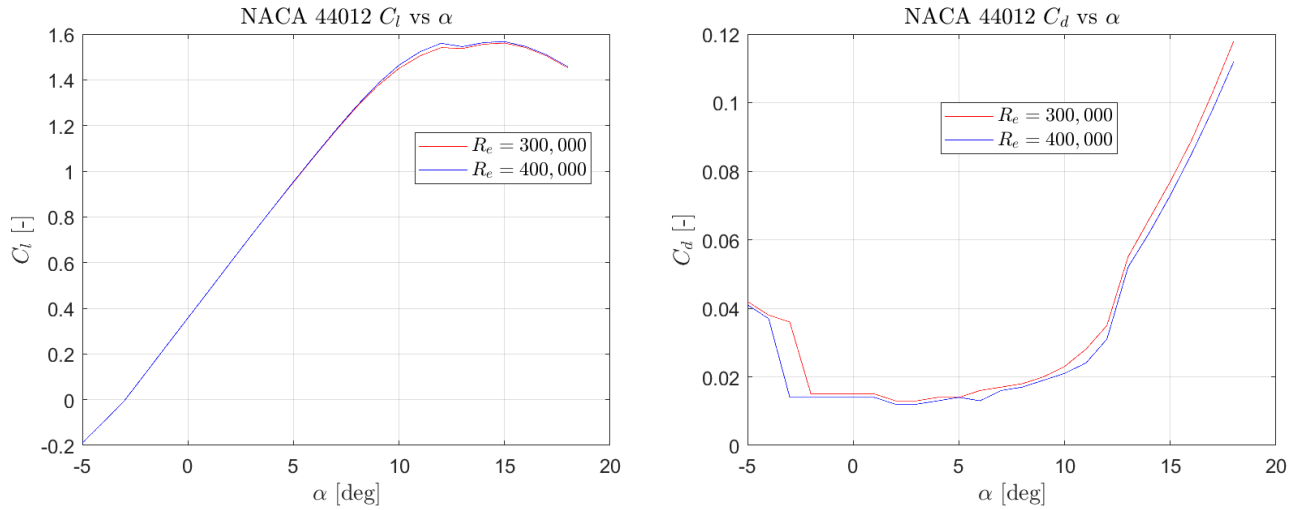

(a) C_l vs α curve. **(b)** C_d vs α curve.

Figure 2.11: NACA 23012 C_l and C_d vs α curves.

Where it can be seen that the 2D lift curve presents a positive non-zero lift value at $\alpha = 0°$, which is coherent with the curvature of this profile and a linear evolution of this coefficient is obtained until the stall region, which appears at $\alpha_{stall,2D} = 14°$ with $C_{l_{max}} \approx 1.90$. The slope of the linear range is C_{l_α} and it can be approximated to $2\pi\, rad^{-1}$. In the other hand, an increasing tendency of the drag coefficient with the angle of attack is obtained, as one could expect.

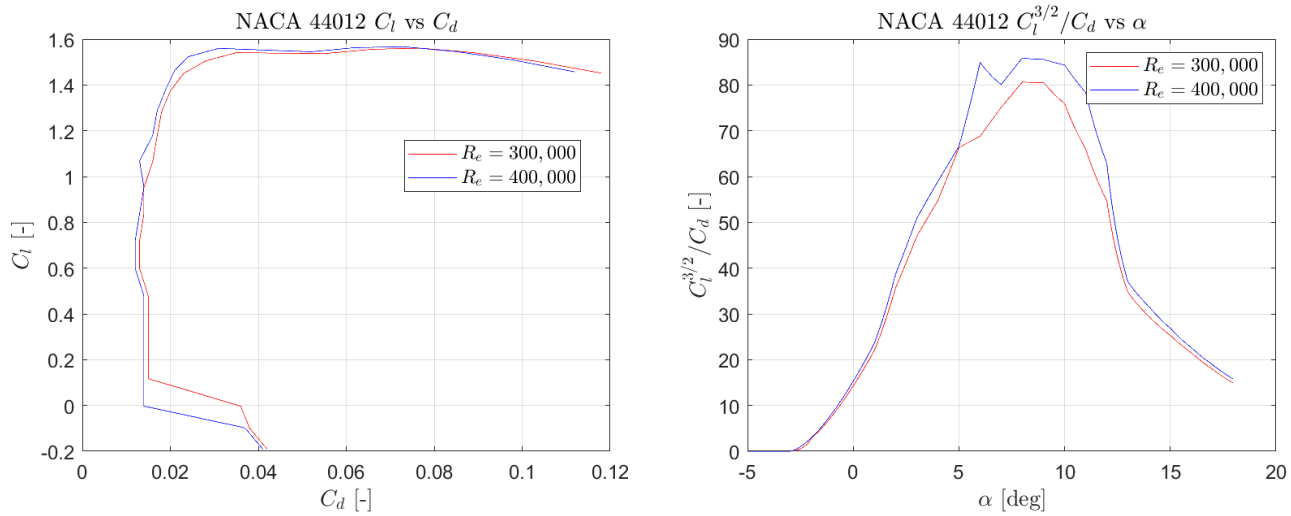

(a) C_l vs C_d curve. **(b)** $C_l^{3/2}/C_d$ vs α curve.

Figure 2.12: NACA 23012 drag polar (a) and endurance parameter (b) curves.

As in Figure 2.12 (b), it is interesting to represent the endurance parameter $C_l^{3/2}/C_d$ (from Equation 2.1 [3]) in function of the AoA. Derived from the Breguet equation for

endurance (which is proportional to the aerodynamic efficiency), it will be an important equation for this thesis, since one of the main objectives of the new design is to achieve a similar endurance as the original ScanEagle. For subscript i referring to the time instant:

$$E = -\int_{W_{i+1}}^{W_i} \frac{\eta_{prop}}{C} \frac{1}{V} \frac{C_L}{C_D} \frac{dW}{W} dt = -\int_{W_{i+1}}^{W_i} \frac{\eta_{prop}}{C} \sqrt{\frac{\rho S_w}{2}} \frac{C_L^{3/2}}{C_D} \frac{dW}{W^{3/2}} dt \tag{2.1}$$

where the velocity V has been substituted from the lift force equation, being $L = W$.

$$V = \sqrt{\frac{W}{1/2\ \rho S_w C_L}} \tag{2.2}$$

One must not forget that, for now, no aspect ratio effects are taken into account. Thus, only two-dimensional C_l and C_d are considered. In the same figure, an optimal AoA for endurance is obtained at around 9°.

Then, the most relevant information about the selected airfoil is presented in Table 2.4:

Feature	**NACA 44012**
$C_{l_{max}}$	1.57
C_{l_α}	0.092 deg^{-1}
$\alpha_{stall,2D}$	15.00 deg
α_{0L}	-2.98 deg
t_{max}	0.12 c_w
x_{max}	0.20 c_w

Table 2.4: NACA 44012 relevant data.

Where t_{max} is the maximum thickness with respect to the chord length and x_{max} the longitudinal position of the maximum thickness with respect to the chord length.

V-tail's airfoil: NACA 0012

For the V-tail, a symmetrical airfoil is going to be selected. Since no pitching nor yawing moments with respect to the center of gravity of the aircraft are desired when the control surfaces are set at zero AoA in level flight.

The airfoil selected, then, is the NACA symmetrical airfoil with the same maximum thickness as the main wing's, the NACA 0012.

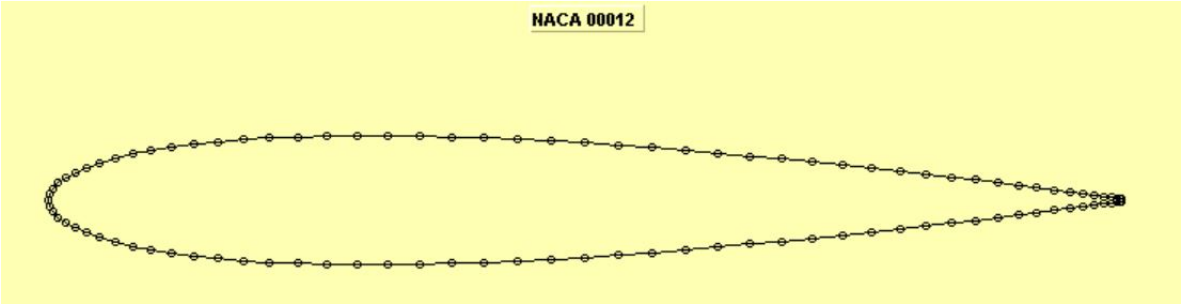

Figure 2.13: NACA 0012 airfoil (JavaFoil).

As a comparison, the $C_l - \alpha$ and $C_d - \alpha$ curves are plotted. In Figure 2.14 (a), it is shown that NACA 0012 airfoils have zero-lift at 0° AoA and also have a lower $C_{l_{max}}$ than the NACA 44012. Although, their linear slopes are identical.

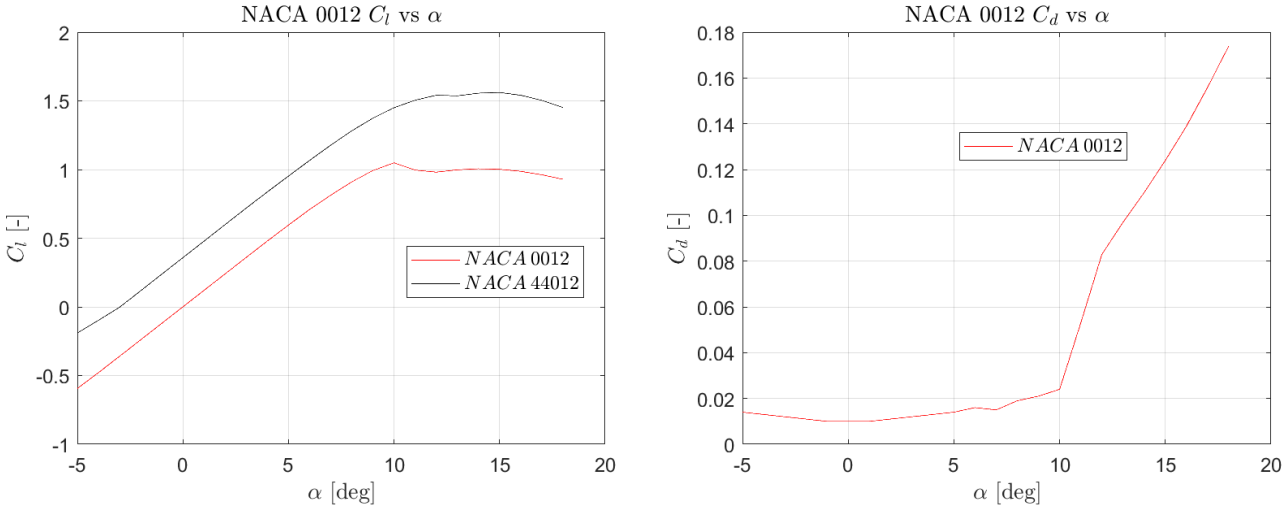

(a) C_l vs α curve.

(b) C_d vs α curve.

Figure 2.14: NACA 0012 C_l and C_d vs α curves ($R_e = 4,000,000$).

And the most relevant information about this airfoil is shown in Table 2.5

Feature	NACA 0012
$C_{l_{max}}$	1.05
C_{l_α}	0.12 deg^{-1}
$\alpha_{stall,2D}$	10.00 deg
α_{0L}	0 deg
t_{max}	0.12 c_w

Table 2.5: NACA 0012 relevant data.

2.4 Estimation of wing lift-related coefficients

From the wing's 2D airfoil (NACA 44012) information, the 3D wing lift-related coefficients can be obtained:

Knowing that:

$$C_L(\alpha) = C_{L_\alpha} \cdot \alpha + C_{L_{\alpha=0}} \tag{2.3}$$

The slope of the linear section can be obtained as:

$$C_{L_\alpha} = \frac{2\pi\ AR}{2 + \sqrt{4 + (AR\ \beta)^2 \cdot \left[1 + tan\left(\frac{\Lambda_{LE}^2}{\beta^2}\right)\right]}} \tag{2.4}$$

Where the sweep angle is in rad and $\beta = \sqrt{1 + M_{eff}^2}$, being $M_{eff} = M_{cr} \cdot cos(\Lambda_{LE})$.

And the lift coefficient for $\alpha = 0°$ can be obtained as:

$$C_{L_{\alpha=0}} = -C_{L_\alpha} \cdot \alpha_{0L} \tag{2.5}$$

On the other hand, the maximum (3D) lift coefficient C_{Lmax} can be obtained analytically.

According to Raymer:

$$C_{L_{max}} = C_{l_{max}} \cdot \frac{C_{L_{max}}}{C_{l_{max}}} + \Delta C_{L_{max}} \tag{2.6}$$

Where the unknown parameters $C_{L_{max}}/C_{l_{max}}$ and $\Delta C_{L_{max}}$ can be obtained knowing the geometry of the wing and looking at the figures described in Raymer's methodology [26].

Then, the maximum angle of attack for which the 3D wing stalls (α at $C_{L_{max}}$) is calculated as:

$$\alpha_{stall} = \frac{C_{L_{max}}}{C_{L_\alpha}} + \alpha_{0L} + \Delta\alpha_{stall} \tag{2.7}$$

Where, again, the unknown parameter $\Delta\alpha_{stall}$ is obtained knowing the wing geometry and looking at the figures from Raymer's methodology.

Finally, the lift coefficient at cruise conditions can be already calculated as in Equation 2.23. To sum up, all the relevant 3D wing lift-related coefficients are presented in Table 2.6:

Parameter	Value
C_{L_α}	$0.082\ deg^{-1}$
$C_{L_{\alpha=0}}$	0.097
$C_{L_{max}}$	1.38
α_{stall}	$16.87\ deg$

Table 2.6: Original ScanEagle lift-related coefficients.

As expected, the 3D wing stalls at a higher AoA than the 2D airfoil with a lower linear slope, but reaches a lower maximum lift coefficient due to the effect of the aspect ratio (see Table 2.4).

2.5 Estimation of weights

It is important to divide the aircraft into its basic components and look for their weights. In this particular case, the conceptual design requires to know the empty weight, payload, fuel and maximum takeoff weights.

For both the reverse engineering and the new design calculations, the payload weight selected will be fixed to $W_{PL} = 5\ kg$, considering that no expendable payload is needed for the mission. This means, the rest of the available weight (taking into account the empty weight as well) that the aircraft will carry until the $MTOW$ restriction, is going to be only fuel.

This will allow to increase the powered endurance and range. It will be also assumed that, at takeoff, $W_{to} = MTOW$. The weight distribution is summarized in Table 2.7:

Element	Weight [kg]
W_{struc}	11
W_{extra}	2
W_{tank}	1.5
W_{eng}	1.5
$\mathbf{W_{empty}}$	**16**
W_{fuel}	5.5
W_{PL}	5
$\mathbf{W_{to}}$	**26.5**

Table 2.7: Original ScanEagle weight estimations [21].

2.6 Estimation of weight fractions

Weight fractions for the whole mission profile may be determined using the prior weight estimates. Depending on the phase of the flight, q different amount of fuel will be burned. These adjustments are important for the calculations since many parameters are affected by the weight evolution of the aircraft.

As previously said, the mission profile is quite straightforward and divided into various sections. The fuel utilized in any of those phases may be stated as the ratio of the end weight over the beginning one (in kg). The goal is to calculate what proportion of the total available fuel weight is spent throughout each phase, allowing to determine the aircraft's performance in terms of endurance and range.

- **Takeoff [1]**: For engine start-up and takeoff, Raymer proposes a weight fraction loss of about 3%. However, since the UAV is launched from the catapult, almost no fuel burn is needed. Considering that $W_{to} = W_1$.

$$\frac{W_2}{W_1} = 0.995 \tag{2.8}$$

- **Climb [2]**: After takeoff, the aircraft has to reach the desired cruise altitude and accelerate (if needed) to the optimal cruise speed. In this phase, the fuel weight lost with respect to the total fuel weight is considered to be a 2%.

$$\begin{aligned} W_2 &= 0.995 \cdot W_1 = 26.37\, kg \\ \frac{W_3}{W_2} &= 0.98 \end{aligned} \tag{2.9}$$

- **First Cruise [3]**: During the cruise to the mission, 320 km are travelled. It is important to know what is the weight of the aircraft at the beginning of this phase ($in = initial$).

$$W_{3,in} = 0.98 \cdot W_2 = 25.84\, kg \tag{2.10}$$

- **Loiter/Mission [4]**: While in the mission area, the UAV will remain airborne as long as there is enough fuel to get back to the origin site.

- **Second Cruise [5]**: The cruise back to the origin site will involve another 320 km, of which a high percent of that distance will be done by a powered flight. The aircraft will start descending when there is only a 5% fuel remaining ($fi = final$). This extra fuel will be reserved for any possible inconvenient.

$$W_{5,fi} = W_1 - 0.95 \cdot W_{fuel} = 21.28\, kg \tag{2.11}$$

- **Descent/Landing [6]**: The whole descent from the cruise altitude will be done gliding, so a lower percentage of those 320 km distance will imply no fuel consumption.

$$W_6 = W_{5,fi} = 21.28\, kg \tag{2.12}$$

2.7 Cruise weight and velocity evolution

As said before, the velocity during First Cruise (phase 3) and the Second Cruise (phase 5) will be that of maximum range. During the Mission (phase 4), the aircraft velocity will be that of maximum endurance.

For programming purposes, the powered mission profile that involves phases 3, 4 and 5 (cruise and mission without gliding) will be divided into 500 steps. The whole calculation will be looped so, when there is convergence, there is always information about which step belongs to the end of phases 3, 4 and 5.

Since this is a loop, at the beginning of each iteration there is information about the engine's SFC at each step, from the previous iteration. The same happens with the endurance obtained. This allows obtaining the weight of the aircraft at the end of phases 3, 4 and 5.

So a weight evolution vector of size 500 can be defined with linear decreasing weight knowing the steps at which the velocity is changed from maximum range to maximum endurance and vice-versa.

Concerning the velocity vector, it also has size 500 and varies knowing that:

$$V = \sqrt{\frac{W \cdot g}{1/2\,\rho\, S_w\, C_L}} \tag{2.13}$$

And C_L is obtained differently depending on the velocity profile. For a **propeller-driven engine** [26]:

$$\begin{aligned} C_{L_{maxR}} &= \sqrt{\frac{C_{D_0}}{k_{ind}}} \quad \text{phases 3 and 5} \\ C_{L_{maxE}} &= \sqrt{\frac{3\,C_{D_0}}{k_{ind}}} \quad \text{phase 4} \end{aligned} \tag{2.14}$$

2.8 Estimation of wing drag

From all the information collected, some basic aerodynamics can be extracted. This is, calculating the drag contributions from the main components and also the lift produced at cruise. As Corke states on his procedure, based on the flat plate analogy, the drag coefficient for the wing can be calculated as:

$$C_D = C_{D_0} + C_{D_i} + C_{D_{visc}} \tag{2.15}$$

where:

- C_{D_0} is the base (zero-lift) drag coefficient.
- $C_{D_i} = k_{ind}\, C_L^2$ represents the induced (due to lift) drag coefficient.
- $C_{D_{visc}} = k_{visc}\,(C_L - C_{L_{minD}})$ is the additional drag term that results from viscous losses, such as those produced by flow separation.

Base drag coefficient

This coefficient can be estimated with the geometrical parameters. So that:

$$C_{D_0} = C_f \cdot F \cdot Q \cdot \frac{S_{wet}}{S_w} \tag{2.16}$$

Where:

- C_f is the skin friction coefficient that depends on the Reynolds number. It is based on the longitudinal development length of the boundary layer and the Mach number. For laminar flow conditions in cruise:

$$C_f = \frac{1.328}{\sqrt{R_e}} \tag{2.17}$$

being $\sqrt{Re} = \sqrt{\frac{V \cdot c_{mac}}{\nu}} < 1000$. So it is laminar according to Corke's method.

- F is the form factor and depends on the geometry of the airfoil:

$$F = \left[1 + \frac{0.6}{(x_{max}/c)} \left(\frac{t_{max}}{c}\right) + 100 \left(\frac{t_{max}}{c}\right)^4\right] \left[1.34\, M_{cr}^{0.18}\, cos(\Lambda_{c/4})^{0.28}\right] \tag{2.18}$$

- Q is the interference factor, that depends on the components that may be attached to the wing or fuselage, disturbing the flow. For high-wing aircraft:

$$Q = 1 \tag{2.19}$$

- S and S_{wet} are the wing surface and the wetted wing surface, respectively. Knowing the shape of the airfoil and the wing surface, the wetted surface can be estimated analytically and should be slightly larger than two times the wing surface. For $t_{max}/c > 0.05$:

$$S_{wet} = S \left[1.977 + 0.52 \left(\frac{t_{max}}{c}\right)\right] \tag{2.20}$$

Induced drag coefficient

For calculating this coefficient, it is necessary to obtain the induced drag parameter and the (3D) lift coefficient.

- The induced drag parameter is calculated as:

$$k_{ind} = \frac{1}{\pi\, AR\, e_{eff}} \tag{2.21}$$

where the Oswald efficiency has been calculated considering the V-Tail/winglet effect according to DATCOM and Scholz et al. [25] as follows:

$$\begin{aligned} e &= \frac{1.1\,(C_{L_\alpha}/AR_w)}{k_{suc}(C_{L_\alpha}/AR_w) + \pi(1-k_{suc})} \\ e_{eff} &= e \cdot \left(\frac{b_{w_{eff}}}{b_w}\right)^2 \end{aligned} \tag{2.22}$$

and, at the same time, k_{suc} is the leading edge suction parameter and it is equal to 0.965, obtained from DATCOM charts using the ScanEagle's basic geometry. The parameter $b_{w_{eff}} = b_w + b_{winglet}$ and C_{L_α} can be already calculated as in Equation 2.4.

- The lift coefficient can be calculated in cruise knowing that $L = W$. As follows:

$$C_L = \frac{W \cdot g}{q\, S_w} \tag{2.23}$$

Viscous drag term

In order to obtain the viscous losses, the minimum-drag lift coefficient and the viscous constant have to be obtained:

- The viscous constant is dependent on the leading-edge radius and taper ratio. It is ranged $0.02 - 0.16$. For a blunt leading edge but relatively high-swept wing, a reasonable value could be $k_{visc} = 0.06$.
- The minimum-drag lift coefficient can be easily obtained as:

$$C_{L_{minD}} = \sqrt{\frac{C_{D_0}}{k_{ind}}} \tag{2.24}$$

Wing drag force and drag coefficient

Once all drag-related coefficients are obtained, the wing drag force and drag coefficient in cruise conditions are:

$$\begin{aligned} C_D &= C_{D_0} + k_{ind}\, C_L^2 \;+\; k_{visc}\,(C_L - C_{L_{minD}}) \\ D &= q\, S_w\, C_D \end{aligned} \tag{2.25}$$

2.9 Estimation of fuselage drag

This base drag estimation follows a similar procedure to the previous one. But, in this case, it is based on an integration along the fuselage length since it is not a perfect cylinder and the flow properties may be different depending on the location. The fuselage is divided into N individual parts and the drag is estimated for each of those parts. The resulting drag force, then, is summed up.

However, since ADS® provides the fuselage wetted area from the 3D model, no integration is going to be needed. The total fuselage drag coefficient is then calculated as:

$$C_{D_f} = C_{D_{0f}} = C_f \cdot F \cdot Q \cdot \frac{S_{f,wet}}{S_w} \tag{2.26}$$

Note that this drag coefficient is normalized with the wing surface. All the parameters within the expression are calculated the same way as in the wing's base drag calculations except for the form factor (F).

- For the friction coefficient (C_f), in this case, the Reynolds number is calculated taking the fuselage diameter (d_f) as the characteristic length. The interference factor (Q) is equal to the unit for a high-wing configuration and $S_{f,wet} = 0.96\, m^2$ according to ADS®.
- The form factor is calculated as:

$$F = 1 + \frac{60}{(1/\delta)^3} + \frac{(1/\delta)}{400} \tag{2.27}$$

  Where $\delta = d_f/l_f$, the so-called fuselage fineness ratio. In order to calculate the fuselage drag force in cruise conditions:

$$D_f = q\, S_w\, C_{D_f} \tag{2.28}$$

2.10 Estimation of V-Tail drag

For the V-Tail, the exact same procedure as the one used for the main wing's base drag is going to be followed, but using the tail's geometry instead. In cruise conditions, the aircraft is assumed to be trimmed longitudinal-wise with no lateral-directional turns.

Thus, no drag effects due to lift are going to be considered for the tail. The more realistic situation would be to consider a slow turn every so often (since the UAV is flying in circles over a certain region), but this situation is going to be neglected.

So the V-Tail's only drag contribution to the total drag will be:

$$D_t = q\, S_w\, C_{D_t} \tag{2.29}$$

Where, again, the tail's drag coefficient is $C_{D_t} = C_{D_{0t}}$ and it is normalized with the main wing's surface. According to Raymer, a tail surface with a hinged rudder or elevator (ruddervator in this case) will have a form factor (F) about 10% higher than predicted by Equation 2.18 due to the extra drag of the gap between the tail surface and its control surface.

2.11 Drag summary

As the propeller is located on the very aft part of the fuselage, it is a pusher system and its dimensions do not largely overpass the fuselage diameter, its drag contribution to the total drag is also going to be neglected[5].

In order to summarize, all the drag-related results will be shown in Table 2.8 (mean values over 500 steps):

Wing	**Fuselage**	**Tails**
$C_{D_0} = 0.0052$	$C_{D_0} = 0.0033$	$C_{D_0} = 0.0009$
$C_{D_i} = 0.0241$	$D_f = 0.826\ N$	$D_t = 0.243\ N$
$C_{D_{visc}} = 0.0030$		
$k_{ind} = 0.0250$		
$C_D = 0.0324$		
$D_w = 7.495\ N$		
Wing only		
$C_{D_0} = 18.70\%\ C_{D_w}$	$C_{D_i} = 72.43\%\ C_{D_w}$	$C_{D_{visc}} = 8.87\%\ C_{D_w}$
Total (aircraft)		
	$C_{D_{tot}} = 0.0367$	
	$D_{tot} = 8.564\ N$	
$C_{D_w} = 87.14\%\ C_{D_{tot}}$	$C_{D_f} = 9.93\%\ C_{D_{tot}}$	$C_{D_t} = 2.93\%\ C_{D_{tot}}$

Table 2.8: IC ScanEagle drag-related results.

[5] in comparison with the main contributors, e.g: main wing, fuselage.

Attending to the summary above, it is interesting to see that the main contributor to the wing's drag is the induced component. Several ways for reducing this term can be approached, such as, increasing the AR and V. Nevertheless, the aircraft weight will have a significant importance since it is directly related to the amount of lift needed. The more lift needed, the higher the induced drag term will be. The goal is, then, to reduce the weight as much as possible to increase the endurance. This will be a compromise between decreasing the induced drag term (thus, the total drag) and keeping an acceptable aerodynamic efficiency at the same time ($AE = \frac{CL}{CD(CL)}$).

On the other hand, as one could expect, the main wing's drag is the main contributor to the total aircraft drag, followed by the fuselage's and then by the V-Tail's drag, which is almost negligible in comparison with the drag the main wing will produce.

2.12 Estimation of propulsion system

As mentioned before, the original ScanEagle is powered by a $1.12\,kW$ piston engine, that drives the propeller and supplies power to the onboard equipment. The most relevant information about the propulsion needed is gathered in Table 2.9.

Feature	**Data**
Fuel type	kerosene
$P_{max}(SLS)$	$1120\,W$
$P_{available}(cruise)$	$673\,W$
P_{PL}	$150\,W$
η_{prop}	0.83
d_{prop}	$0.41\,m$
pi_{prop}	$0.36\,m$
C_P	0.129
C_T	0.082
J	0.944
$SFC(SLS)$	$9.00 \cdot 10^{-4}\,kg/Wh$
SFC	$SFC(Mach, T)$

Table 2.9: Original ScanEagle propulsion estimations [35].

The needed power, then, is distributed into the shaft power to the propeller and the different payload users, which demand a power equal to P_{PL} just while the UAV is on the mission area (phase 4 only). These users can be avionics, full motion sensor, anti-icing system, camera or other necessary accessories [28].

As the total drag of the UAV has been already estimated, some calculations on the engine can be performed. Assuming that the aircraft has to counteract the total drag force in cruise flight, and estimating a realistic propeller efficiency, the shaft power in W needed is:

$$P_{sh} = \frac{D_{tot} \cdot V}{\eta_{prop}} \tag{2.30}$$

In order to obtain the needed power at each step, the constant P_{PL} has to be added to the shaft power needed during the mission (phase 4 only).

$$P_{needed} = P_{sh} + P_{PL} \tag{2.31}$$

In the other hand, the power available at the cruise altitude (constant) can be estimated knowing the maximum power at SLS and the air density at that altitude [29]:

$$P_{available} = P_{max} \cdot \frac{\rho}{\rho_{SL}} \tag{2.32}$$

For the SFC evolution (Model X [7]), a reference (sea level) value, Mach number and ambient temperature at both cruise altitude and sea level must be known (see Table 2.9). Where the Mach number at sea level has been estimated so that the resulting average velocity is the same as the average cruise velocity.

$$SFC = SFC_{SL} \cdot \sqrt{\frac{M \cdot T}{M_{SL} \cdot T_{SL}}} \tag{2.33}$$

The engine's rotational speed at every step can be calculated using the following equation [36]:

$$\omega_{prop} = \sqrt[3]{\frac{P_{needed}}{k_{prop} \cdot d_{prop}^4 \cdot pi_{prop}}} \tag{2.34}$$

where pi_{prop} (pitch), d_{prop} (diameter) are expressed in inches and $k_{prop} = 5.30 \cdot 10^{-5}$ to provide ω_{prop} in rpm.

From propeller engines, 3 relevant non-dimensional parameters can be obtained. In cruise:

- The power coefficient

$$C_P = \frac{V_{cr}}{\omega_{prop}^3 \cdot d_{prop}^5} \tag{2.35}$$

- The thrust coefficient

$$C_T = \frac{P_{sh}}{\rho_{cr} \cdot \omega_{prop}^2 \cdot d_{prop}^4} \tag{2.36}$$

- The advance ratio

$$J_{prop} = \frac{V_{cr}}{\omega_{prop} \cdot d_{prop}} \tag{2.37}$$

2.13 Estimation of performance

Now that all the needed parameters for calculating the performance of the aircraft are estimated, some relevant results can be obtained.

- Wing loading ($L = W \cdot g$):

$$WL = \frac{W \cdot g}{S_w} \tag{2.38}$$

- Stall speed:

$$V_{stall} = \sqrt{\frac{W \cdot g}{1/2\ \rho\ S_w\ C_{L_{max}}}} \tag{2.39}$$

  Where, at every step, it has to be checked that the aircraft velocity is always at least 10% higher than V_{stall}. This is where a good airfoil selection gains importance.

- Aerodynamic efficiencies:

$$\begin{aligned} AE_{max} &= \frac{1}{2\sqrt{C_{D_0} \cdot k_{ind}}} \\ AE &= C_L/C_D \end{aligned} \tag{2.40}$$

- Powered Endurance in hours (Breguet eq.):

$$E = \sum_i^{500} \frac{AE_i}{C_i} \cdot ln\left(\frac{W_i}{W_{i+1}}\right) = \mathbf{16.76\ h} \tag{2.41}$$

Where $C_i = \frac{SFC \cdot V}{550 \cdot \eta_{prop}} \cdot g \cdot \frac{lbm2kg}{lbf2N}$. Where, according to Corke, $SFC\,[lb/(hp \cdot h)]$, $V\,[ft/s]$ and $\frac{lb2kg}{lbf2N}$ is the corresponding unit conversion so that endurance is in h.

- Powered Range in kilometers (Breguet eq.):

$$R = \sum_{i}^{500} E_i \cdot V_i \cdot \frac{3600}{1000} = \mathbf{2005.30\,km} \tag{2.42}$$

- Extended Range (gliding) in kilometers:

$$\begin{aligned} \gamma_{glide} &= atan(\frac{1}{AE_{max}}) = 0.029\,rad = 1.70^{\circ} \\ R_{glide} &= \frac{z_{cr}}{tan(\gamma_{glide}) \cdot 1000} = \mathbf{168.31\,km} \end{aligned} \tag{2.43}$$

Where z_{cr} is in m.

- Extended Endurance (gliding) in hours:

$$E_{glide} = \frac{R_{glide}}{cos(\gamma_{glide}) \cdot V \cdot \frac{3600}{1000}} = \mathbf{1.41\,h} \tag{2.44}$$

Where $V\,[m/s]$ and AE_{max} are constant during all the gliding descent and are equal to their corresponding values at the last step of the powered flight (step 500). The gliding range R_{glide} is in km.

- Total Endurance and Range:

$$\begin{aligned} E &= \mathbf{18.17\,h} \\ R &= \mathbf{2173.60\,km} \end{aligned} \tag{2.45}$$

According to the results above, the obtained endurance is close enough to what it was found in the literature. Thus, the reverse engineering procedure can be considered for the new design.

For better comprehension, several parameter evolutions during the powered flight will be plotted:

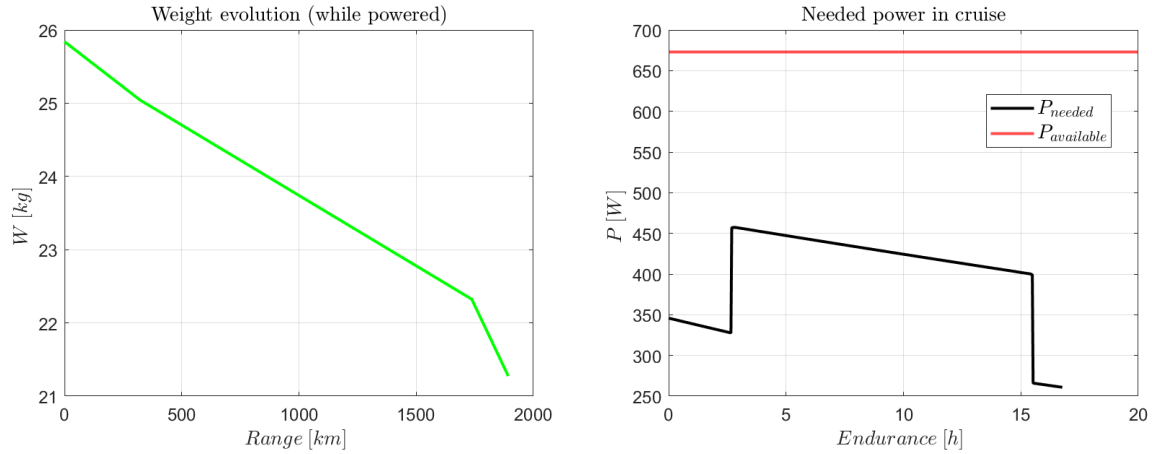

(a) Original Weight vs Range evolution. **(b)** Original Power needed in cruise.

Figure 2.15: Reverse engineering parameter evolutions (I).

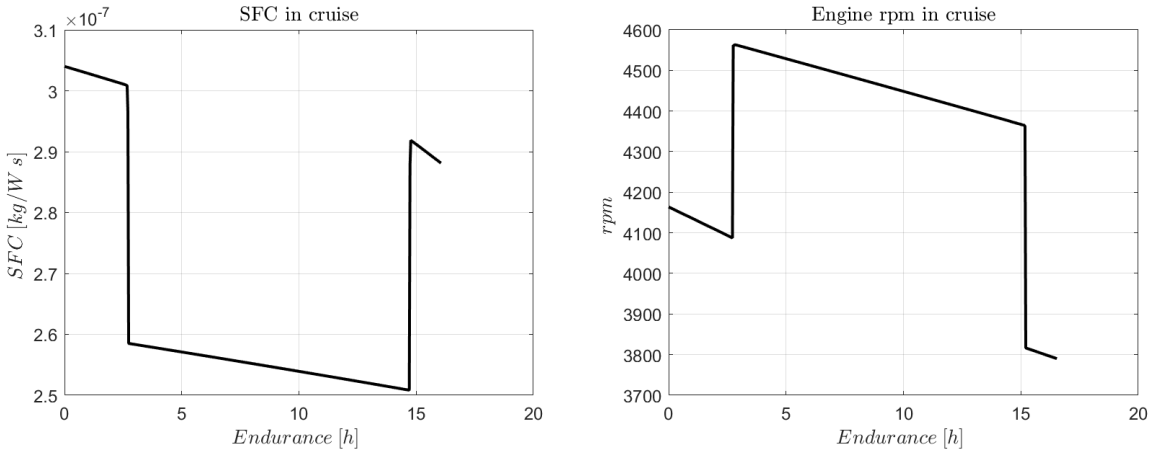

(a) Original SFC during cruise. **(b)** Original rpm during cruise.

Figure 2.16: Reverse engineering parameter evolutions (II).

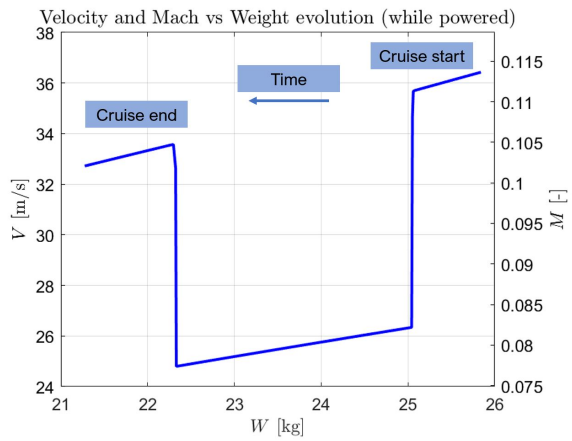

(a) Original Velocity and Mach vs weight evolution.

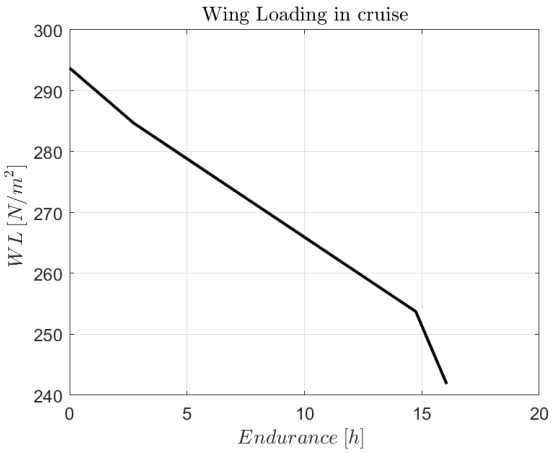

(b) Original Wing loading during cruise.

Figure 2.17: Reverse engineering parameter evolutions (III).

Where, in all of the figures above, a decreasing tendency in time/range can be seen because of the fuel weight loss. Sudden variations in those evolutions are due to the switch in maximum range and endurance velocity profiles.

In Figure 2.15b, the power needed in cruise is always lower than the maximum power available at the cruise altitude. In the other hand, payload power during the mission implies in average a 50% increase in the needed power.

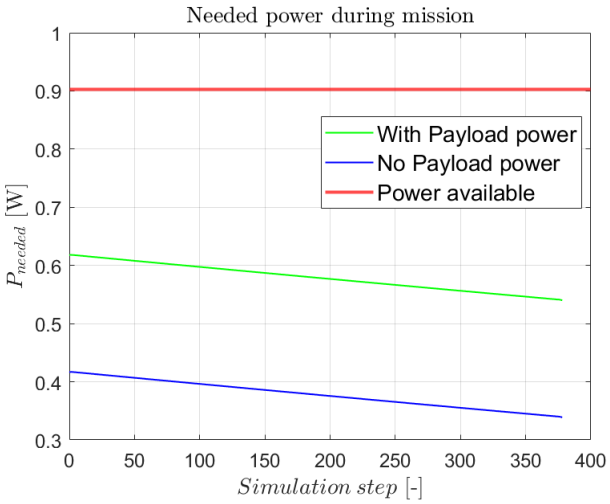

Figure 2.18: Original needed power versus payload power during mission.

2.14 Sensitivity analysis

To finalize the reverse engineering process, a sensitivity analysis will be performed. This is, modifying some parameters by a certain percentage and compare the effects produced with respect to the original geometry. The more significant the relative variation, the more sensitive the parameter will be. Doing this, the dominant parameters are identified and the new design can be developed in convenience.

This sensitivity analysis is shown in Table 2.10, where the major or most relevant relative variations are highlighted.

	AR $+15\%$	**b** $+15\%$	$\mathbf{d_f}$ $+15\%$	$\mathbf{l_f}$ $+15\%$	$\mathbf{W_{to}}$ $+15\%$
Dimensions					
S_w [%]	+13.56	+32.25	+0.00	+0.00	+0.00
$Fin.ratio\ (\delta)$ [%]	+0.00	0.00	+15.00	−13.04	+0.00
Drag					
AE [%]	+8.74	+2.90	+0.51	+0.53	+1.71
$C_{D_{0w}}$ [%]	−6.54	+2.82	−0.07	−0.07	−2.96
C_{D_i} [%]	−8.55	−7.13	−0.91	−0.98	−3.19
$C_{D_{0f}}$ [%]	−9.17	−19.95	−2.80	−2.86	−4.58
$C_{D_{0vt}}$ [%]	−17.35	−21.58	−0.07	−0.08	−2.96
C_{D_0} [%]	−8.53	−7.08	−0.95	−0.97	−3.48
C_D [%]	−8.32	−7.71	−0.97	−1.02	−3.28
D_{tot} [%]	−8.04	−2.82	−0.51	−0.53	+16.69
Propulsion					
η_{prop} [%]	+0.00	+0.00	+0.00	+0.00	+0.00
C_P [%]	+0.00	+0.00	+0.00	+0.00	+0.00
C_T [%]	+1.35	+6.87	−0.33	−0.34	−1.10
Performance					
E [%]	+15.95	+15.19	+0.17	+0.25	−22.91
V_{stall} [%]	−6.16	−13.04	+0.00	+0.00	+8.94
V_{maxE} [%]	$-6-02$	−10.77	+0.24	+0.24	+9.91
WL [%]	−11.94	−24.29	+0.00	+0.00	+18.68

Table 2.10: Results from the sensitivity analysis.

It is evident that the variations in wingspan come in first place, followed by variations in aspect ratio and aircraft weight. However, it is worth mentioning that a slight increase in fuselage length and diameter has little effect on either performance or aerodynamics.

This is very convenient for the new design because it will probably require modifications in fuselage size.

- **Drag:** The induced drag and the fuselage/tails base drag are the most sensible parameters. To reduce them, it seems like the wingspan has to be increased, thus, the aspect ratio as well, since these parameters are directly proportional. The wing surface would have to be increased accordingly to achieve this goal. But this also implies that the aircraft weight will be inevitably increased, compromising this solution.

  However, the total drag is mostly reduced by increasing the aspect ratio while minimizing the weight, only. Since the shaft power is directly proportional to the total drag, the most optimized this tendency is, the less shaft power will be needed in cruise.

  So there has to be an equilibrium between a large wingspan, aspect ratio and a low weight. Fortunately, the fuselage length and diameter can be increased without major penalty, but considering that this would potentially contribute to increasing the weight too.

- **Propulsion:** Regarding propulsion, no major modifications are shown. Except for the fact that the power needed would be modified in accordance to the total drag (see Equation 2.30). However, this power strongly depends on the selected propulsion system, which will be certainly modified.

- **Performance:** To boost the endurance (and the aerodynamic efficiency), the same procedure for optimizing the total drag applies.

To sum up, the sensitivity analysis suggests that, for decreasing the total drag force (D_{tot} and all drag coefficients) and increasing the aircraft's endurance (E), the wingspan (b_w) and the aspect ratio (AR) have to be increased, while minimizing the aircraft's takeoff weight (W_{to}). These results will be helpful as a starting point for the drone's initial sizing.

Chapter 3

The FC ScanEagle

In this chapter, the new design is going to be implemented according to the objectives described in Chapter 1 - section 3 and the results obtained from the IC ScanEagle reverse engineering. The major modification is to implement an electrical engine that is mainly powered by a *PEMFC hydrogen fuel cell*. Since batteries are not optimal for long endurance applications due to their weight and low power capacity, a PEMFC can be a better option. In this type of system, electrical power will be generated continuously as long as there is available hydrogen and oxygen. It is more efficient in terms of power-to-weight capability than the batteries available on the market.

The PEMFC is referred as the aircraft's main power source because it will not be the only one. In fact, the addition of a battery would be a complementary solution for providing a considerable power boost for a short period of time. This means, the UAV will use a battery for the climbing phase, in which the available power provided by the fuel cell may not be sufficient.

The fuel cell is the core of the power generating system, but several other components are necessary to keep the fuel cell operating effectively and to guarantee reaction products exit the system appropriately. Figure 3.1 is an example of integrating a fuel cell stack as a power generator for a propellant application. Wet air is supplied with hydrogen via the anode to the fuel cell in this setup. The water vapor produced as a byproduct at the cathode output is utilised in the humidifier before the absorbed air is discharged into the environment. Finally, the fuel cell stack not only powers its application but may also power the other system components.

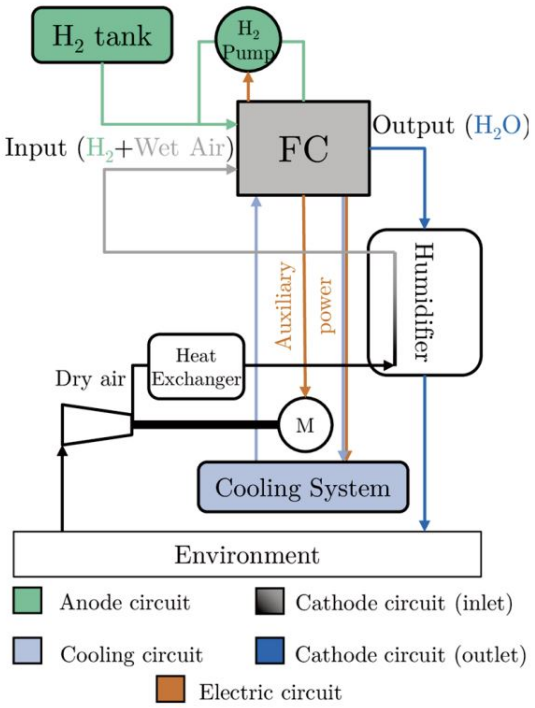

Figure 3.1: Fuel cell system outline integrating the FC stack and the components of the balance of plant [12].

Whereas the whole powerplant system scheme is shown in Figure 3.2:

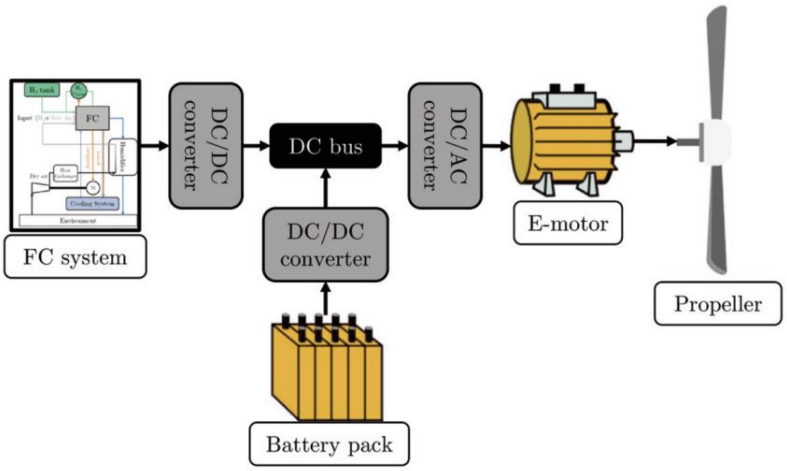

Figure 3.2: Powerplant components outline [23].

1 The PEMFC

The hydrogen fuel cell will be the main propulsion device. This technology is still relatively new and has been steadily developing over the past few decades. However, further research on PEMFC performance is out of the scope of this thesis. As a matter of fact, the drone's power requirements will rely on the fuel cell state of the art.

1.1 Working principle

A fuel cell is a device that uses a chemical reaction between oxygen and hydrogen fuel to turn stored molecular energy into electrical energy. Anode, cathode, and an electrolyte membrane make up the cell itself (see Figure 3.3).

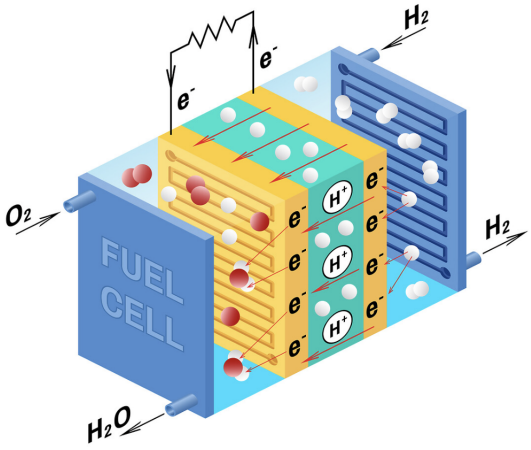

Figure 3.3: Proton Exchange Membrane Fuel Cell scheme [2].

The anode is where hydrogen enters the fuel cell. Hydrogen atoms react with a catalyst and divide into electrons and protons in this reaction. On the other side, oxygen from the surrounding air enters through the cathode. The positively charged protons travel to the cathode via the porous electrolyte membrane. The negatively charged electrons exit the cell and generate an electric current, which can be utilized to power an electric motor. Protons and oxygen combine to form water vapor in the cathode, which is the only emission produced [2].

In the case of hydrogen, the reactions are, in general [1]:

[1]Depending on the type of fuel cell used, based on its architecture and the electrolyte, the reactions vary. This chemical formula is related to solid oxide fuel cells and was selected for simplicity.

$$\begin{aligned} \text{Anode: } & H_2 \rightarrow 2H^+ + 2e^- \\ \text{Cathode: } & O_2 + 4e^- + 4H^+ \rightarrow 2H_2O \\ \text{Overall: } & 2H_2 + O_2 \rightarrow 2H_2O \end{aligned} \tag{3.1}$$

However, for most purposes, fuel cells cannot be made up of merely an anode/cathode pair (single cell), because the electrical power generated would be insufficient. That is why they create a compound system known as a "stack" in which they are arranged in consecutive layers, boosting the overall power output of the system.

2 Sizing methodology

The approach used to accomplish the adaptation will be extensively discussed when the initial conditions for the model are specified using the related sources. The major features to adapt will be the new characteristics for the structure, fuel cell, fuel storage system, battery and electrical motor. Starting with the mission definition and instances to be studied, the focus will transition to a schematic overview of the many steps of the iterative methods, the data utilized to accomplish the estimation, and the logic underpinning the decision-making. Following a broad description of the technique, a deeper dive into the mathematical models, assumptions, and ramifications of each stage of the element dimensioning will be made.

2.1 Iterative procedure overview

The sizing of the new design will start with the original IC ScanEagle geometry (Table 2.3) and weights (Table 2.7). Then, the process will be composed of three dependent loops. The first, known as the **geometry loop** from this point on, focuses on changing the wing loading needed in cruise to obtain the required endurance at a certain cruise altitude and speed ($25 - 35\ m/s$), as well as modifying the wingspan and wing surface accordingly. The fuselage length and width will be updated so the fuel tank, battery and fuel cell can fit inside.

Once completed, the **cruise loop** will be used to iteratively compute the fuel reservoir characteristics required to finish the mission given the components indicated for that iteration, settling a provisional mass of the aircraft for a particular fuel and tank mass.

The third loop, known as the **climb loop**, will utilize the previous results to estimate

the power necessary to climb at a certain rate with the previously determined weight distribution and decide if the power supplied to the aircraft is sufficient to complete the stated maneuver. The electric motor power will be modified as a result of this. Additionally, the battery size will be calculated since so it can provide the difference between the required and the supplied power by the fuel cell system. Given the revised size of these elements, the weight of the entire aircraft will be updated, and therefore the structure and subsequently cruise power will require new modifications, repeating the entire process iteratively, as shown in Figure 3.4.

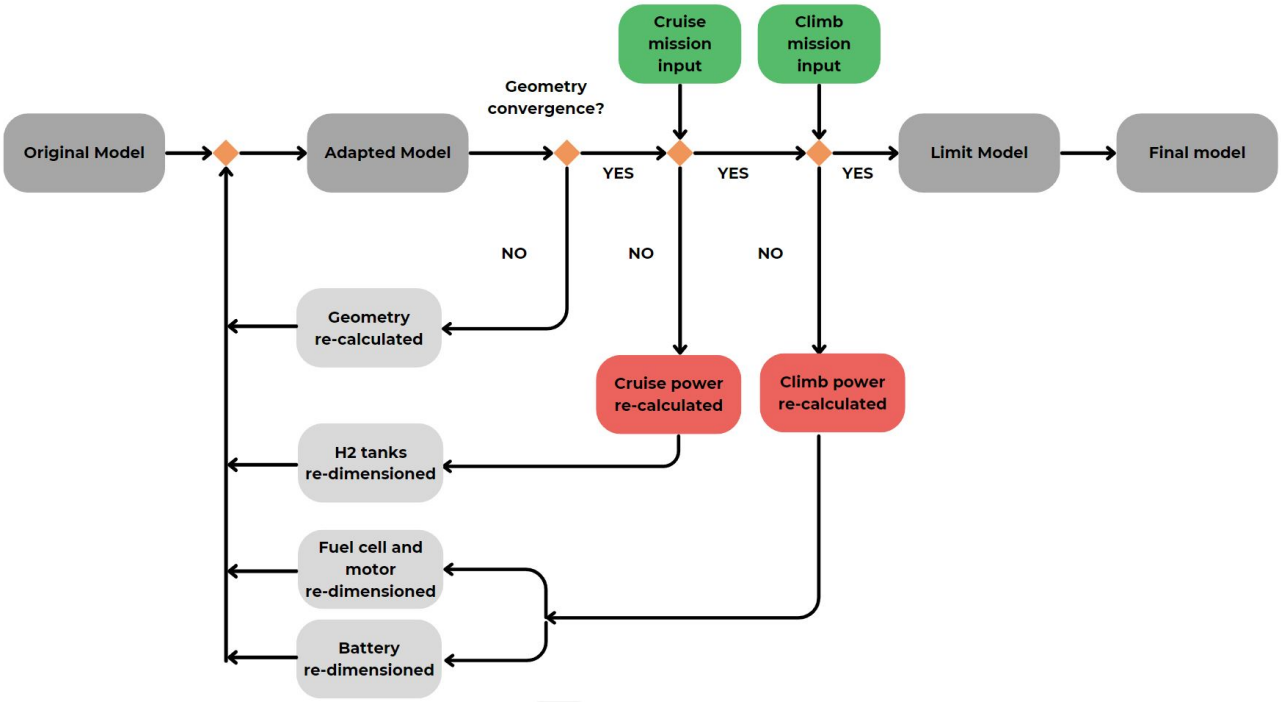

Figure 3.4: Flowchart of the overall procedure followed to perform the UAV adaptation.

Where, the *Adapted model* collects the updated power system, fuel storage and battery requirements and simulates the entire mission as in the reverse engineering, the *Limit model* fulfills the mission objectives within several versions and the *Final model* is ultimately selected as the optimal Fuel Cell ScanEagle among the possible versions.

2.2 Geometry loop

The geometry loop consists in selecting initial aerodynamic parameters (C_{D_0}, k_{ind}) and a reference S_w and b_w. A design cruise velocity is also selected so that the output results provide reasonable values for the geometry. The wing loading needed at the cruise altitude for a C_L that maximizes endurance is then calculated as:

$$WL = \frac{W \cdot g}{S_w} = \frac{1}{2}\rho V^2 \sqrt{\frac{C_{D_0}}{k_{ind}}} \tag{3.2}$$

Then, weight fractions for the mission are estimated as in the reverse engineering, knowing the SFC in cruise (obtained at the previous iteration). This loop ends when the difference in wing surface between iterations is lower than $0.01\,m^2$. It is important to mention that the main wing's aspect ratio may be increased in order to obtain the desired endurance. And also the taper ratios are kept as in the original design.

The output results for this loop are:

- Provisional cruise wing loading (WL)
- Provisional aerodynamic parameters (C_{D_0}, k_{ind}, AE)
- Updated geometry ($b_w, S_w, l_f, d_f, S_{f,wet}$)

2.3 Cruise loop

The cruise loop is mainly used for selecting the PEMFC, dimensioning the fuel tank and estimating the amount of fuel needed in order to perform the mission.

Hydrogen storage

The decision of using a *Type IV*[2] cylindrical tank pressurized at $700\,bar$ is made. Since it is a common way of storing gaseous hydrogen in similar applications. In order to obtain the amount of fuel and the mass and volume of the tank, hydrogen's Lower Heating Value, density and the gravimetric capacity of the tank at that pressure are needed:

Property	**Value (700 bar)**
LHV_{H_2}	$33.33\,kWh/kg$
ρ_{H_2}	$42\,kg/m^3$
$C_{g,tank}$	$1.4\,kWh/kg$

Table 3.1: Hydrogen storage relevant information [14].

[2]This tank consists of a thin ($5mm$) liner made of high density polyethylene (HDPE)

Cruise powers and SFC

Knowing the maximum shaft power (payload power included in loiter) needed in cruise from the last iteration (P_{needed}), other powers can be obtained. These powers are the electrical and the fuel cell powers. Each one of them can be calculated knowing the corresponding efficiencies of both the electric motor and the fuel cell. Knowing this, the PEMFC is selected so it can provide enough power even in the worst case scenario, which is already considered since the shaft power in cruise selected is the maximum obtained in the mission simulation.

$$\begin{aligned} P_{needed} &= D_{tot} \cdot V/\eta_{prop} \\ P_{elec} &= P_{needed}/\eta_{mot} \\ P_{fc} &= P_{elec}/\eta_{fc} \end{aligned} \tag{3.3}$$

In order to obtain P_{fc} from P_{elec}, a procedure to obtain η_{fc} has to be followed:

1. Find the corresponding polarization curve from the fuel cell manufacturer (see Annex section 1).

2. Multiply the number of cells times the ideal voltage ($1.23\,V$).

3. Dividing the net power (P_{elec}) obtained, over the multiplied voltage, search for the needed current. This current corresponds to a new voltage in the polarization curve.

4. The fuel cell efficiency at sea level is obtained dividing the last voltage obtained graphically and the one calculated knowing the number of cells and the ideal voltage.

5. To estimate a new fuel cell efficiency considering the altitude, an efficiency drop constant can be obtained graphically from [23] in Figure 3.5.

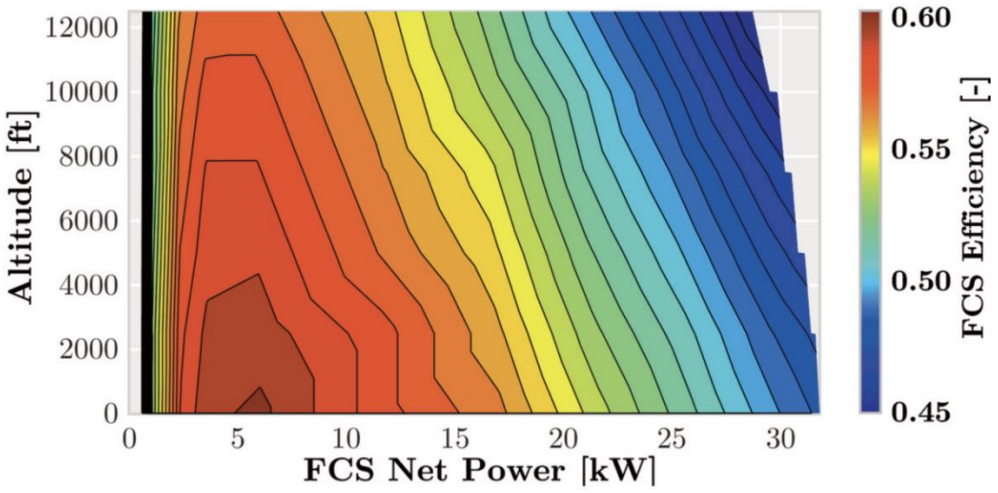

Figure 3.5: Net power vs fuel cell efficiency at different altitudes for a 40 kW fuel cell [23].

On the other hand, knowing hydrogen's LHV, the aforementioned efficiencies and the DC/DC inverter efficiency ($\approx 95\%$), the SFC $[kg/(W \cdot s)]$ in cruise can be estimated as:

$$SFC = \frac{1}{LHV_{H_2} \cdot \eta_{prop} \cdot \eta_{mot} \cdot \eta_{fc} \cdot \eta_{DCDC}} \tag{3.4}$$

Fuel tank sizing

Once all the previous information is calculated, the mass of fuel can be estimated knowing the cruise flight endurance, as follows:

$$\begin{aligned} \dot{m}_{fuel} &= P_{fc}/LHV_{H_2} \\ W_{fuel} &= \dot{m}_{fuel} \cdot E \\ v_{fuel} &= W_{fuel}/\rho_{H_2} \end{aligned} \tag{3.5}$$

For the tank's mass and volume, the corresponding gravimetric and volumetric capacities from Table 3.1 are used:

$$\begin{aligned} W_{tank} &= W_{fuel}/(C_{g,tank}/LHV_{H_2}) \\ v_{tank} &= v_{fuel} \end{aligned} \tag{3.6}$$

2.4 Climb loop

Climb loop is used for the battery and electric motor dimensioning as well as for updating the aircraft's takeoff weight by means of assigning an individual weight for each component.

Battery power storage

The decision is to opt for a High-Voltage Cathod Lithium NCM 622 battery. Which are widely produced and have reasonable gravimetric and volumetric energy densities for this kind of application.

Property	Value
$C_{g,bat}$	$0.22\,kWh/kg$
$C_{v,bat}$	$0.60\,kWh/L$

Table 3.2: Battery power storage relevant information [6].

Battery and electric motor sizing

In order to estimate the amount of power that the battery has to supply during the climb phase, the excess power ($P_{av} - P_{req}$) has to be calculated knowing the rate of climb and a provisional takeoff weight.

$$\begin{aligned} V_{climb} &= \frac{P_{av} - P_{req}}{W_{to} \cdot g} \\ P_{req} &= 1.10 \cdot (P_{needed} + W_{to} \cdot g \cdot V_{climb})/(\eta_{prop} \cdot \eta_{mot}) \end{aligned} \tag{3.7}$$

Where P_{req} is the required power for the ascent, in which the change in potential energy is added to the needed power in cruise and increased in a 10% so the calculation is more conservative. As the power that the battery needs to supply is electrical, the result is divided by the propeller and the electric motor efficiencies.

The available power (P_{av}) is the one provided by both the fuel cell and the battery at the same time. And it is also used to size the electric motor, this time not considering electrical power but mechanical. The motor mass will be estimated as an exponential

correlation ($R^2 = 0.99$) of *mgm Compro* electric motors' catalogue [9]. Where the mass of the motor as function of peak power follows the ecpression:

$$W_{mot} = 2.2761e^{0.0325P_{mot_{max}}} \tag{3.8}$$

Then, the power needed for the battery can be obtained knowing the available power for the climb rate selected and the maximum electric power that the fuel cell will need provide in cruise. It is important to take into account that the battery has an efficiency of about 90% and it cannot be fully discharged, thus, a 20% discharge margin is considered. Once the climb rate is selected, the time needed for ascending to the cruise velocity can be easily obtained, providing the energy needed for the battery.

$$\begin{aligned} P_{bat} &= (P_{av} - P_{elec})/\ (\eta_{bat}) \\ J_{bat} &= P_{bat}(1.20 \cdot t_{climb}) \end{aligned} \tag{3.9}$$

Finally, the energy needed for the battery during the ascent is obtained. Its mass and volume can be calculated using the data in Table 3.2.

$$\begin{aligned} W_{bat} &= J_{bat}/C_{g,bat} \\ v_{bat} &= J_{bat}/C_{v,bat} \end{aligned} \tag{3.10}$$

2.5 Updated takeoff weight

At the end of the iteration, the aircraft weight is updated, knowing the mass of each component, as in Table 3.3. The only components that will remain constant with the same weight as in the original design are the auxiliary elements (W_{extra}) and the payload (W_{PL}). The structural weight will vary depending on how the geometry is modified for a certain design.

Component	Weight
W_{struc}	Modified by geometry
W_{extra}	$2\,kg$
W_{fc}	Modified by cruise and FC
W_{tank}	Modified by cruise and FC
W_{mot}	Modified by climb
W_{bat}	Modified by climb
$\mathbf{W_{empty}}$	
W_{fuel}	Modified by cruise and FC
W_{PL}	$5\,kg$
$\mathbf{W_{to}}$	

Table 3.3: Weight distribution for the FC ScanEagle by component.

It is important to mention that the structural factor for the FC ScanEagle may increase considerably, since the major contributions to the total weight of the aircraft correspond to the empty weight (mainly structure, fuel tank and battery). This is due to the fact that hydrogen fuel mass will be noticeably decreased compared to kerosene and the payload weight will remain constant and relatively lightweight. Obviously there is no crew weight involved, so the structural factor is even larger than the already high IC ScanEagle's ($s = 0.60$).

To compute the structural weight, a conservative approximation will be done considering the increment in wingspan and fuselage length. Since the is no enough bibliography corresponding to the estimation of UAV structural weight, a linear estimation from the results obtained by [11] using the aircraft conceptual design software known as AAA will be done. As the authors stated, the drone's structural weight may not follow a linear tendency as the takeoff weight increases. For this reason, the estimation performed can be considered as conservative and may also account for the V-tail's structural mass increase as well. The linear correlations obtained for the total increase in structural weight both wingspan and fuselage are:

$$\begin{aligned} W_{b_w} &= 2.7485 \cdot b_w - 4.8762 \\ W_{l_f} &= 3.442 \cdot l_f - 0.1817 \end{aligned} \tag{3.11}$$

In order consider the net weight increase, the original masses of these structures must be subtracted (3.60 and 5.40 kg, respectively).

2.6 V-tail sizing

As a first approximation, the V-tail geometry will be kept as in the original *IC ScanEagle*, but as the endurance and takeoff weight requirements increase, the control surface's area variation cannot be neglected. The coefficient C_t in Equation 3.12 is usually derived from literature, but in this case a very specific arrangement (twin vertical stabilizers over the main wing that also perform as winglets) is used and very little information can be obtained from UAV correlations so that the precision of the calculations can be trusted.

$$S_t = C_t \frac{b_w S_w}{l_t} \tag{3.12}$$

Where l_t is the distance from the main wing's and tail's aerodynamic centers. This implies that C_t should be retro-engineered as it may differ noticeably from the conventional (manned) geometry aircraft.

However, the V-tail geometry must account for both lateral and longitudinal stabilities, which are related to a preliminary stage of the design. The decision, then, is to approximate this provisional geometry as a proportional increment in wing surface. Keeping the same surface ratio between the V-tail's and main wing's areas from the original design. It is also important to consider a large enough V-tail span so that the ScanEagle can be captured by the *SkyHook* system at landing. This feature strongly depends on the aircraft's landing weight, geometry and the *SkyHook's* capabilities themselves.

3 Simulation cases

Once the design procedure is known, several simulations can be performed in order to analyze different versions of the *FC ScanEagle*, depending on the cruise altitude, climb rate and target endurance.

The simulation cases or drone versions selected are the following ones:

- **CASE 1:** $z_{cr} = 5000\,m$, $V_{climb} = 2\,m/s \rightarrow t_{climb} = 41.67\,min$, $E \approx 18\,h$
- **CASE 2:** $z_{cr} = 3000\,m$, $V_{climb} = 2\,m/s \rightarrow t_{climb} = 25.40\,min$, $E \approx 18\,h$
- **CASE 3:** $z_{cr} = 3000\,m$, $V_{climb} = 4\,m/s \rightarrow t_{climb} = 12.70\,min$, $E \approx 18\,h$
- **CASE 4:** $z_{cr} = 5000\,m$, $V_{climb} = 2\,m/s \rightarrow t_{climb} = 41.67\,min$, $E \approx 10\,h$
- **CASE 5:** $z_{cr} = 3000\,m$, $V_{climb} = 2\,m/s \rightarrow t_{climb} = 25.40\,min$, $E \approx 10\,h$

The mission selected will be exactly as for the original *ScanEagle* (see Figure 2.7). In which the same distances and velocity profiles in cruise for reaching the mission site and back to the origin site will be assumed. The simulation steps will be kept the same as well, in order to compare the performance of every fuel cell drone design with the internal combustion one.

4 Results

After applying the sizing methodology explained in section 2 for all five cases, the results shown in Table 3.4 were obtained. The decisions for those cases were made so that all objectives stated for this thesis were considered. Results show that not all of them can be accomplished at the same time for a single case or version. Mainly due to the fact that:

- The cruise altitude severely influences the aircraft's takeoff weight (via climb velocity) and geometry, compromising the ability for the new design to be adapted to the takeoff and landing procedures of the original *ScanEagle*.
- The aircraft's takeoff weight and geometry directly influences the performance capabilities in terms of endurance and range.

For this reason, each of these five versions can be selected for a specific requirement, that must consider some (but not all) of the initial mission objectives:

- **CASE 1:** It is the heaviest version, that requires the heaviest equipment (empty weight) and demands the largest geometry (wingspan, fuselage length, etc.) in order to accomplish the initial target endurance. On the other hand, takeoff and landing procedures will certainly have to be reconfigured for this version to be correctly adapted to them.

- **CASE 2:** In order to accomplish the target endurance reducing the drone's size and takeoff weight, the original cruise altitude had to be lowered. Potentially compromising the drone's detectability. This version keeps a balance between a reasonable takeoff weight and endurance.

- **CASE 3:** Similar to *CASE 2*, but with a reduced ascent time, compromising the aircraft's weight and size (because of the climb-dependent elements, e.g. battery and motor) while reaching the target endurance.

- **CASE 4:** This version can fly at the original cruise altitude, reducing the takeoff weight and size by lowering the target endurance. Which may be an interesting alternative for those missions that require less loiter time. Takeoff and landing procedures must be assessed in a similar way as *CASES 2* and *3*.

- **CASE 5:** Similar approach to *CASE 4*, but lowering both the original cruise altitude (as in *CASES 2* and *3*) and the target endurance (as in *CASE 4*). This is the lightest and most compact version of all five. Which would be the one that can could be adapted the best to the original takeoff and landing procedures while compromising detectability and loiter time during mission.

Parameter	CASE 1	CASE 2	CASE 3	CASE 4	CASE 5
Efficiencies					
η_{prop}	0.83	0.83	0.83	0.83	0.83
η_{DCDC}	0.95	0.95	0.95	0.95	0.95
η_{mot}	0.90	0.90	0.90	0.90	0.90
η_{fc}	0.59	0.58	0.58	0.59	0.58
η_{bat}	0.90	0.90	0.90	0.90	0.90
Powers, Energy					
$P_{needed}\,[W]$	762	540	620	622	502
$P_{elec}\,[W]$	846	600	690	691	558
$P_{fc}\,[W]$	1424	1033	1188	1163	962
$P_{fc_{rated}}\,[W]$	2000	1200	1200	1200	1200
$P_{av}\,[W]$	4669	3275	6326	3530	2787
$P_{req}\,[W]$	3234	2272	4137	2472	1959
$P_{mot_{max}}\,[W]$	4500	3000	6000	3500	3000
$J_{bat}\,[kWh]$	3.54	1.51	1.59	2.62	1.51
Geometry					
AR_w	14.60	14.60	14.60	14.60	14.60
$b_w\,[m]$	7.38	5.11	5.46	6.10	4.43
$l_f\,[m]$	4.06	2.81	3.00	3.35	2.44
$d_f\,[m]$	0.47	0.33	0.35	0.39	0.28
Weights, Volumes					
$W_{fc}\,[kg]$	3.00	2.15	2.15	2.15	2.15
$W_{fuel}\,[kg]$	0.77	0.56	0.64	0.35	0.29
$W_{tank}\,[kg]$	18.30	13.27	15.28	8.30	6.87
$v_{tank}\,[L]$	18.30	13.27	15.28	8.30	6.87
$W_{bat}\,[kg]$	16.08	6.86	7.23	11.95	5.72
$v_{bat}\,[L]$	5.89	2.66	2.76	4.38	2.10
$W_{mot}\,[kg]$	2.63	2.51	2.77	2.55	2.51
$W_{struc}\,[kg]$	26.42	18.58	20.94	25.53	17.37
$W_{empty}\,[kg]$	68.43	45.37	50.37	50.48	36.52
$W_{to}\,[kg]$	74.20	50.93	56.01	55.83	41.91
s	0.92	0.89	0.90	0.90	0.87
Performance					
$E\,[h]$	18.3	16.8	18.1	11.0	10.3
$R\,[km]$	2167	2127	2167	1361	1319

Table 3.4: Results obtained for five versions of the *FC ScanEagle*.

4.1 Weight distribution overview

Weight distribution comparisons between models can be helpful to obtain trends depending on mission requirements. In Figure 3.6, the weight distribution of the most relevant elements of the aircraft in the form of a bar chart can be seen, for every fuel cell version of the drone as well as the original internal combustion one.

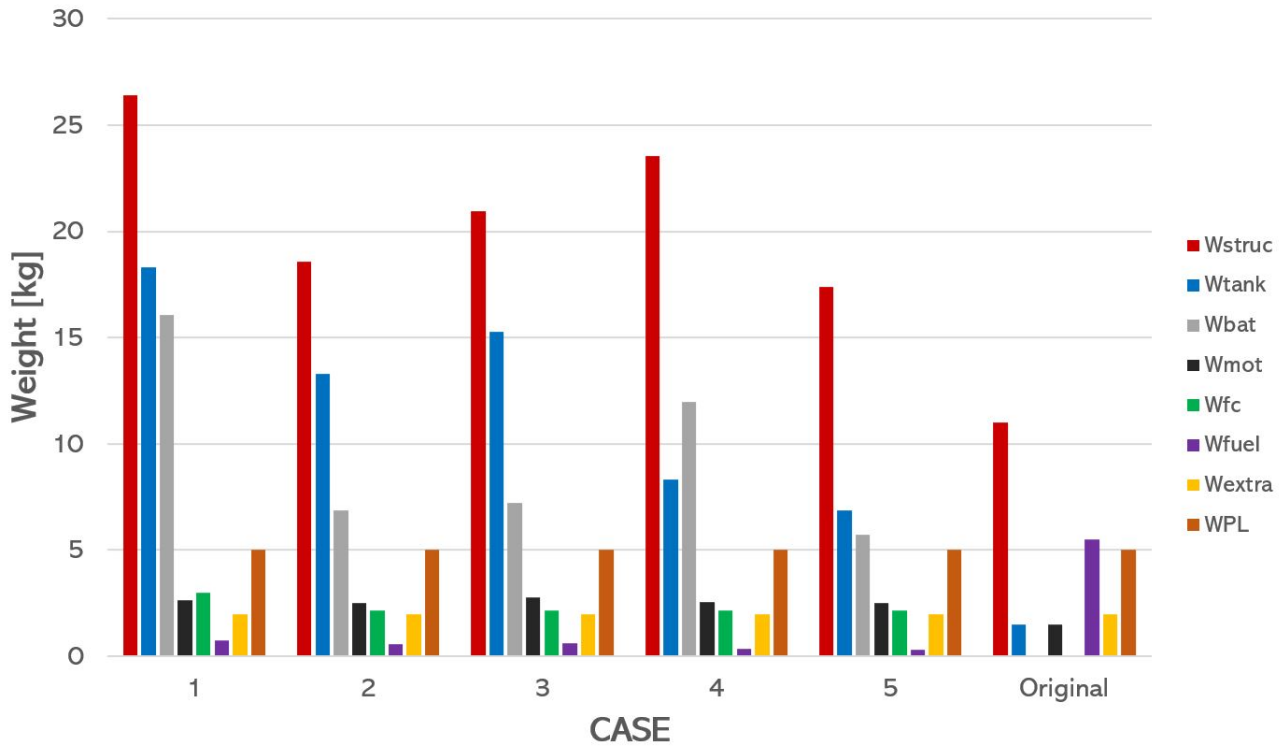

Figure 3.6: Weight distribution of each element for five *FC ScanEagle* versions and original *IC ScanEagle* in kilograms.

Results show that the main individual contributor to the overall weight of the aircraft is the structural weight, in all cases. Fact that may seem logical since it is responsible for the integrity of the drone. However, the main difference between the original design and the fuel cell versions is that the mass of the tank is significantly larger for the fuel cell designs, as one may have predicted in advance, due to the low volumetric energy density of gaseous hydrogen. Increasing the operational empty weight of the aircraft noticeably, specially in long endurance missions. On the other hand, fuel mass is reduced in an order of magnitude compared to the kerosene version because of hydrogen's high specific energy.

Regarding the propulsion system (composed of fuel cell, tank, battery and electric motor), the most relevant fact is that both cruise altitude and climb speed play an important role in battery dimensioning. As it can be seen, the battery weight becomes more relevant

in those cases in which the cruise altitude is higher (*CASES 1* and *4*), due to the amount of energy needed for a certain climb rate. This increment in battery weight can also be observed between *CASES 2* and *3*, in which the only difference in their requirements is the climb velocity. Being this velocity for *CASE 3* doubled with respect to *CASE 2*, the takeoff weight increases around 5 kg, what actually suggests one of the best ways for minimizing weight in this kind of aircraft is reducing the climb rate as much as possible for a certain mission.

The rest of the propulsion system components (fuel cell and electric motor) do not imply a significant change in the operational empty weight due to their lightweight design. However, in the case of the electric motor, the correlation used may introduce an error due to the lack of available information in the market about motors for this kind of application.

In Figure 3.7, the contribution of the aforementioned elements to the total aircraft weight can be seen. This time, considering all four elements of the propulsion system together (W_{propul}). It is interesting to see how the propulsion system mass becomes the main contributor to the total weight for those cases that prioritize endurance as an objective, requiring larger tank sizes. This tendency is yet increased for higher cruise altitudes, in which the battery becomes heavier as well.

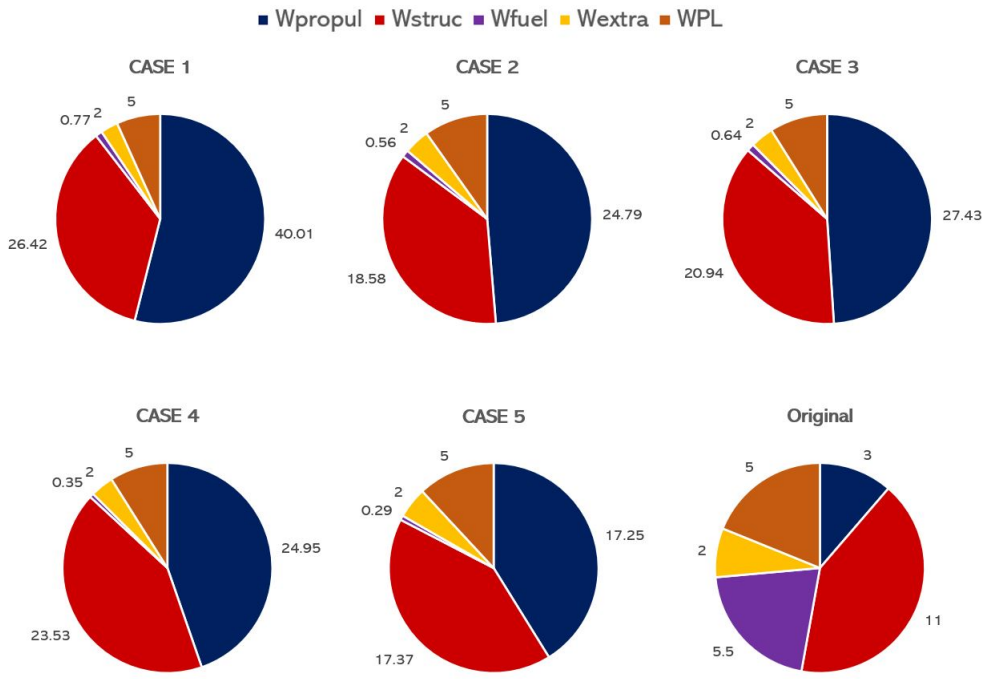

Figure 3.7: Weight contributions to the total weight of each element for five *FC ScanEagle* versions and original *IC ScanEagle* in kilograms.

Structural and propulsion system weights, then, become more balanced for relatively lower endurance missions, even if the cruise altitude differ from one model to the other. For the original design, the relatively lightweight tank and engine make the operational empty weight decrease in comparison to the fuel cell versions. This, combined to the fact that the amount of fuel (kerosene) needed for long endurance missions is quite larger to their fuel cell counterparts, justify the extremely high structural factor of the *FC ScanEagle* ($s \approx 0.90$). For this factor to be decreased, the payload weight has to be increased noticeably, since the hydrogen fuel weight will always be a very small fraction of the total weight.

4.2 Size comparison

For a visual comparison, two other 3D models (*CASES 1* and *5*) in ADS® were done. Figure 3.8 shows the difference in length, width and wingspan of the original *IC ScanEagle*, the most compact and the largest *FC ScanEagle* (CASES 5 and 1, respectively).

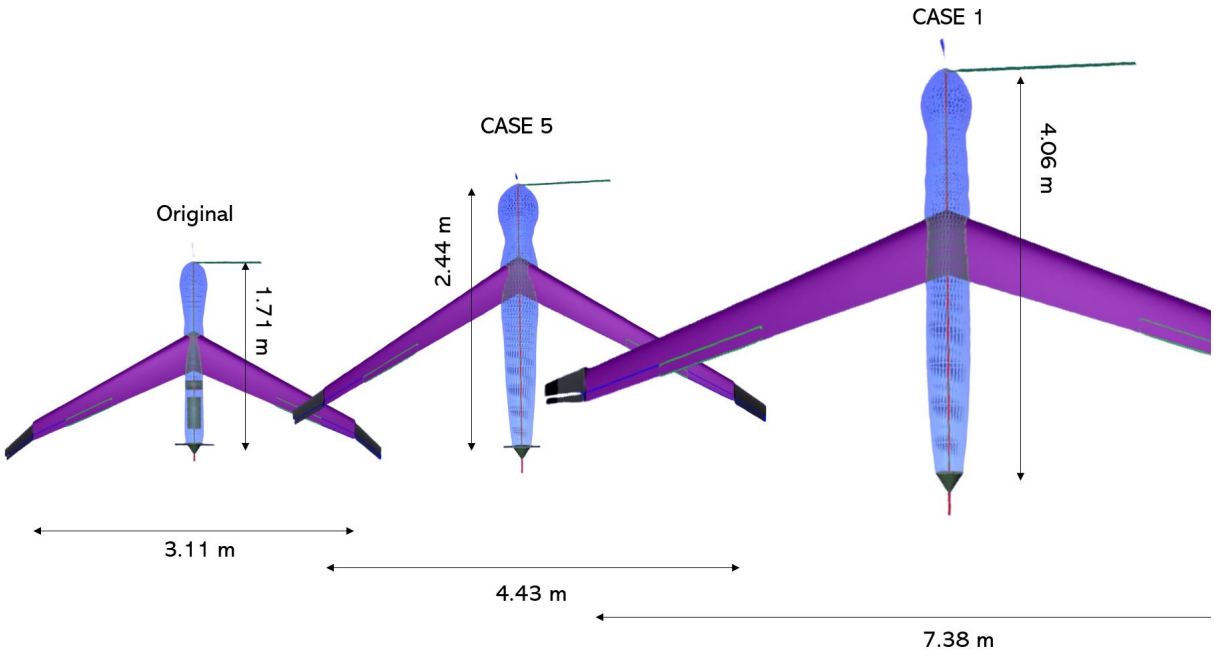

Figure 3.8: Size comparison between the original *IC ScanEagle* (left), CASE 5 *FC ScanEagle* (center) and CASE 1 *FC ScanEagle* (right).

As one can see, *CASE 5* is the best option to be adapted to the takeoff catapult and landing cable due to its geometric similarities to the original drone, compromising two relevant characteristics such as cruise altitude and mission endurance. On the other hand, *CASE 1*, while fulfilling the latter requirements, will most likely be unable to adapt to the

same takeoff and landing procedures due to its large geometry and weight. Which is quite inconvenient to the overall philosophy of the ScanEagle, that one may argue is related to compactness, ease of transport, speed and flexibility in takeoff and landing sites, etc.

Volume adaptation

As the dimensions of the different components that belong inside the fuselage can be obtained analytically or by the manufacturer, their adaptability can be estimated knowing the volume inside the fuselage of the different versions provided by ADS® software.

Assuming that the available space inside the fuselage for installing the needed equipment (tank, battery, electric motor, fuel cell, avionics, cables, pipes, etc.) is around 70% of the total volume the software computes and that the shape of the tank is cylindrical with spherical edges at both sides. The volumes of the propulsion system are summarized in Table 3.5:

Parameter	**CASE 1**	**CASE 5**
$l_f\ [m]$	4.06	2.44
$d_f\ [m]$	0.47	0.28
$v_{bat}\ [L]$	5.89	0.95
$dim_{mot}\ [m]$	$\phi 0.10 \times 0.10$	$\phi 0.08 \times 0.10$
$v_{mot}\ [L]$	0.79	0.50
$dim_{fc}\ [m]$	$0.339 \times 0.143 \times 0.172$	$0.279 \times 0.127 \times 0.143$
$v_{fc}\ [L]$	8.34	5.07
$dim_{tank}\ [m]$	$\phi 0.19 \times 0.53$	$\phi 0.14 \times 0.35$
$v_{tank}\ [L]$	18.30	6.87
$v_{tot}\ [L]$	**33.31**	**14.54**
$v_f\ [L]$	**418**	**120**

Table 3.5: Volumes of each component compared to the total available volume inside the fuselage for *CASES 1* and *5*.

Resulting in more than enough available space inside the fuselage for each component. Even though the structural weight estimation for each version may seem logical, it also may be conservative. That means further studies in fuselage and wing masses are recommended, so that the empty weight of the drone is minimized without compromising its structural integrity. This study could also address the optimization of the fuselage internal volume, but always prioritizing the stability of the aircraft (this belongs to the preliminary stage of the design).

Chapter 4

Conclusions

In this thesis, the aircraft conceptual design theory described by Corke and Raymer has been used in order to conceptually design five versions of a hydrogen powered *ScanEagle* UAV via cruise simulations and an iterative process. The main conclusions obtained after the analysis of the results are the following:

1 Conclusions

The reverse engineering section has been useful not only to find precise magnitudes of the original *ScanEagle's* geometry and performance but also to validate the cruise simulation that involves the aerodynamics, propulsion, and performance of the aircraft at a certain altitude. In addition, the sensitivity analysis suggestion of increasing the main wing's aspect ratio (thus wingspan) to obtain a larger endurance has been followed, which has contributed to improve the performance of the new designs.

For the *FC ScanEagle* versions sizing, several hypotheses have been considered, such as: constant efficiencies for all the components during climb and cruise phases, a 10% increase in the power required during the ascent for conservative purposes, an exponential correlation for electric motor sizing according to the manufacturer's catalogue, a linear correlation for the main wing and fuselage weights and a proportional increase in V-tail surface with the main wing's area. These hypotheses were taken because of the lack of available information about certain components and always staying on the conservative side, penalizing in performance if necessary.

Results show that the initial objectives of the new design cannot be fulfilled all at once for a certain version or case. Mainly due to the fact that fuel cell-powered drones demand

different components for the propulsion system that directly affect their takeoff weight and geometry. Depending on how these objectives are prioritized, a different version of the *FC ScanEagle* may be selected.

As result, according to the original ScanEagle philosophy, the optimal choice might be between *CASES 2* and *5*. On the one hand, *CASE 2* compromises cruise altitude and it is more difficult to be adapted to the original takeoff and landing procedures while keeping the original endurance. On the other hand, *CASE 5* can be better adapted to the latter procedures while also compromising the mission endurance. Turning out that the adaptability to takeoff and landing procedures is the key factor in the decision.

Overall it has been proven that these PEMFC gaseous hydrogen-powered aircraft show promising results. Although these drones have significant disadvantages in terms of endurance and weight, they are nonetheless capable of executing useful missions while emitting no pollutants or CO_2. Meaning this technology is expected to be a viable alternative to internal combustion engines for powering aircraft at least within the unmanned segment. As technology matures and the industry transitions to cleaner energies, hydrogen will reduce its cost and its storage techniques will progressively improve potentially presenting itself as a better alternative to the existing power production methods.

2 Further studies

The successful study of the cases presented for the FC system as a powerplant for a *ScanEagle* drone has opened the door to future research on the subject. This would expand understanding of how fuel cell implementations impact these kind of vehicles, which would aid the advancement of similar technology in this specific area.

Hydrogen propulsion systems in aviation are undergoing significant and growing research subjected to continuous improvement. Today, converting the *ScanEagle* to hydrogen may seem only possible by means of pressurized gas tanks, however, liquid hydrogen storage would allow to save more weight. Before that step, the implementation of more sophisticated tanks (e.g. *Type V* composed by just a CFRP layer) could help improve the performance of the designed models.

A relevant contribution for increasing the performance could be the redesign of the fuselage. In fact, the choice of keeping a constant fuselage section and the same fineness and wingspan-to-length ratio as the original design can be sub-optimal. Thus, an optimization of fuselage structural weight and dimensions is recommended.

Despite the fact that flying at a higher altitude can reduce the skin drag, the climb phase requires a large amount of available power combining the fuel cell and battery, increasing both battery and electric motor weights, counteracting the positive effect of a higher cruise altitude. This fact suggests a better analysis of the optimal cruise altitude so that takeoff weight is minimized within the mission objectives.

It would also be a great addition to this work to compare the carbon emissions of the fuel cell models with the original *IC ScanEagle*, providing more information on the feasibility of this technology within a sector that is increasingly demanding lower carbon footprints, potentially increasing the profitability of this kind of propulsion as it would indicate the advantage that they present, reducing the environmental impact that humans cause.

Finally, the best way of validating the results obtained from this study would be to produce an experimental prototype, whether it is in real life operations or in a testbench. Ultimately confronting the economic and time resources that any of the aforementioned conceptual designs would require.

Annex

H3 Dynamics A-1200 LV 1200 W

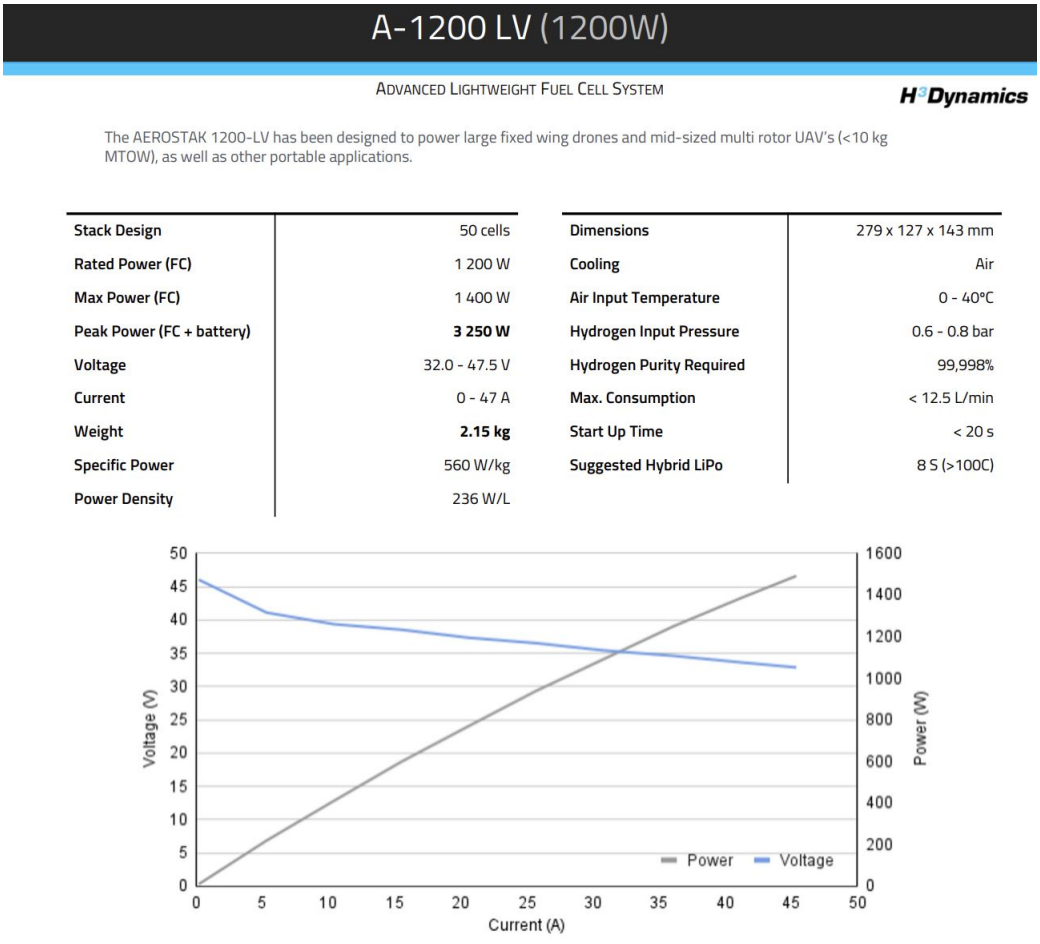

Figure 4.1: H3 Dynamics A-1200 LV 1200 W Fuel Cell [16].

H3 Dynamics A-2000 2000 W

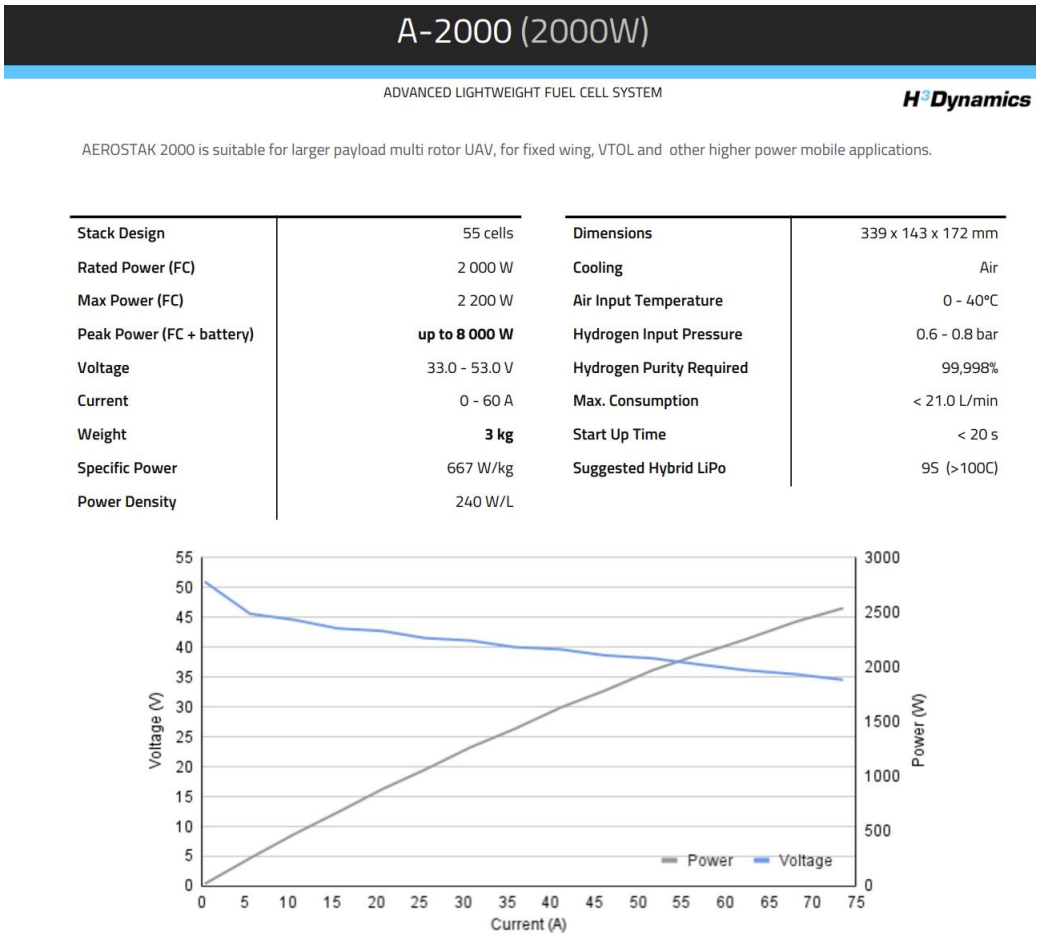

Figure 4.2: H3 Dynamics A-2000 2000 W Fuel Cell [16].

Bibliography

[1] Eric Aaslund et al. "Conceptual design of a Boeing ScanEagle drone with hydrogen and PEMFC". In: *Université Libre de Bruxelles* (2022).

[2] Airbus. *Hydrogen Fuel Cells*. https://www.airbus.com/en/newsroom/news/2020-10-hydrogen-fuel-cells-explained. 2020.

[3] AOE.vt. *Range and Endurance*. https://archive.aoe.vt.edu/lutze/AOE3104/range&endurance.pdf.

[4] Barnardmicrosystems. *Insitu Group scanEagle A-15*. https://barnardmicrosystems.com/.

[5] Military UAS Business News. *Insitu ScanEagle to Compete for Brazilian Maritime ISR Programme*. https://www.uasvision.com/2014/03/28/insitu-scaneagle-to-compete-for-brazilian-maritime-isr-programme/. 2014.

[6] Wenzhuo Cao and Jienann Zhang. *Batteries with high theoretical energy densities*. https://www.sciencedirect.com/science/article/abs/pii/S240582971931102X. -.

[7] Marcos Carreres. "Propulsion models". In: *Universitat Politècnica de València* (2020).

[8] McKinsey Company. "[Hydrogen-powered aviation: A fact-based study of hydrogen technology, economics, and climate impact by 2050]". In: *Mckinsey* (2020).

[9] mgm Compro. *mgm Compro RET DC motors*. https://www.mgm-compro.com/electric-motor/13-kw-electric-motor/. -.

[10] Thomas C. Corke. *Design of aircraft*. Prentice Hall, 2003.

[11] Nicolas Dalmazio et al. "Boeing ScanEagle drone with H2 PEMFC. Using AA Software". In: *Université Libre de Bruxelles* (2022).

[12] José M. Desantes et al. "Feasibility study for a cell-powered unmanned aerial vehicle with a 75 kg payload". In: *Sciendo* (2022).

[13] Doosan. *DJ25*. https://www.doosanmobility.com/en/products/drone-dj25. -.

[14] US Drive. *Hydrogen Sotrage Tech Team Roadmap*. https://www.energy.gov/sites/prod/files/2017/08/f36/hstt_roadmap_July2017.pdf. -.

[15] Drones-Mart. *Eagle Plus UAV VTOL 3500 mm*. http://www.drones-mart.com/product/10052/Eagle-Plus-UAV-VTOL-3500mm. 2014.

[16] H3 Dynamics. *Hydrogen-Electric UAS. Power Solutions and Accessories*. https://www.h3dynamics.com/_files/ugd/3029f7_20bd14d7c2e2474296b8986004002b18.pdf. -.

[17] Enapter. *What is the energy content of hydrogen?* https://www.enapter.com/newsroom/kb_post/what-is-the-energy-content-of-hydrogen. -.

[18] Lorenzo Fiori. *ScanEagle hook*. https://www.researchgate.net/figure/ScanEagle-R-unmanned-aerial-vehicle-UAV-Boeing-Insitu-Bingen-WA-USA-lands-on_fig1_317256965. 2017.

[19] FuelCellsWorks. *MMC UAV Hydrogen Drone*. https://fuelcellsworks.com/news/mmc-uav-hydrogen-drone-breaks-new-record-for-flight-time/. -.

[20] Insitu. *ScanEagle 3*. https://www.insitu.com/products/scaneagle3.

[21] Insitupacific. *Malaysia Receives First Batch of Donated ScanEagle UAVs from US*. https://insitupacific.com.au/systems/scaneagle2/.

[22] MMC. *Griflion M8*. https://www.mmcuav.com/products/griflion-m8/. -.

[23] S. Molina et al. ""Optimization and sizing of a fuel cell range extender vehicle for passenger car applications in driving cycle conditions". In: *Applied Energy* (2021).

[24] Australian Navy. *ScanEagle launched*. https://www.navy.gov.au/unmanned-systems/scaneagle.

[25] M. Nita and D. Scholz. *Estimating the Oswald factor from basic aircraft geometrical parameters*. https://www.fzt.haw-hamburg.de/pers/Scholz/OPerA/OPerA_PUB_DLRK_12-09-10.pdf. 2012.

[26] Daniel P. Raymer. *Aircraft design: A conceptual approach*. American Institute of Aeronautics and Astronautics, 1992.

[27] Researchgate.net. *A Long Range Fuel Cell/Soaring UAV System for Crossing the Atlantic Ocean*. https://www.researchgate.net/publication/336305238_A_Long_Range_Fuel_CellSoaring_UAV_System_for_Crossing_the_Atlantic_Ocean. -.

[28] Defense Studies. *Malaysia Receives First Batch of Donated ScanEagle UAVs from US*. https://defense-studies.blogspot.com/2020/03/malaysia-receives-first-batch-of.html. 2020.

[29] Virginia Tech. *Thrust models*. https://archive.aoe.vt.edu/lutze/AOE3104/thrustmodels.pdf. -.

[30] Naval Technology. *Ion Tiger UAV*. https://www.naval-technology.com/projects/ion-tiger-uav/. -.

[31] Unmanned Systems Technology. *Fuel Cells for Drones UAV*. https://www.unmannedsystemstechnology.com/expo/fuel-cell-systems/. 2022.

[32] Naval Technoology. *Ion Tiger UAV*. https://www.naval-technology.com/s?search=ion+tiger. 2013.

[33] Department of Transportation. Tech. rep. *2-blade propeller*. url:https://rgl.faa.gov. 2014.

[34] Turbosquid. *Professional UAV 3D models*. https://www.turbosquid.com/3d-model/uav.

[35] UAS Vision. *3W-Powered UAV for Flights in Antarctica*. https://www.uasvision.com/2016/07/11/3w-powered-uav-for-dlights-in-antarctica/. 2016.

[36] S. Vorkoetter. *Propeller basics*. http://www.stefanv.com/rcstuff/qf200203.html. -.